A SPARSE CONTROL APPROACH TO OPTIMAL SENSOR PLACEMENT IN PDE-CONSTRAINED PARAMETER ESTIMATION PROBLEMS

IRA NEITZEL, KONSTANTIN PIEPER, BORIS VEXLER, AND DANIEL WALTER

Abstract. We present a systematic approach to the optimal placement of finitely many sensors in order to infer a finite-dimensional parameter from point evaluations of the solution of an associated parameter-dependent elliptic PDE. The quality of the corresponding least squares estimator is quantified by properties of the asymptotic covariance matrix depending on the distribution of the measurement sensors. We formulate a design problem where we minimize functionals related to the size of the corresponding confidence regions with respect to the position and number of pointwise measurements. The measurement setup is modeled by a positive Borel measure on the spatial experimental domain resulting in a convex optimization problem. For the algorithmic solution a class of accelerated conditional gradient methods in measure space is derived, which exploits the structural properties of the design problem to ensure convergence towards sparse solutions. Convergence properties are presented and our findings are compared to previous results. A variational discretization of the continuous problem based on finite elements is investigated and the presented results are confirmed by numerical experiments.

Keywords: PDE-constrained inverse problems, Optimal sensor placement, Sparsity, Conditional gradient methods

AMS Subject Classification: 35R30, 49K20, 62K05, 65K05, 49M25

1. Introduction

In this paper we propose a measure-valued formulation for the optimal design of a measurement setup for the identification of an unknown parameter vector entering a system of partial differential equations. Many applications in physics, medicine or chemical engineering for example rely on complex mathematical models as a surrogate for real-life processes. Typically the arising equations contain unknown (material) parameters which have to be identified in order to obtain a realistic model for the simulation of the underlying phenomenon. To illustrate the ideas, we consider a similar example as presented in [10]. Here, the combustion process of a single substance on a two dimensional domain Ω is modeled by a non-linear convection-diffusion equation with an Arrhenius-type reaction term, depending on four scalar parameters D, E, d, and c, representing its material properties:

$$-\Delta y + \alpha \cdot \nabla y + D \exp\{-E/(d-y)\}\, y(c-y) = 0 \quad \text{in } \Omega, \tag{1.1}$$

together with $y = \hat{y}$ on an inflow boundary $\Gamma_{\text{in}} \subset \partial\Omega$ and $\partial_n y = 0$ on $\partial\Omega \setminus \Gamma_{\text{in}}$. While c and d are known physical constants, the pre-exponential factor D and the activation energy E are empirical and cannot be measured directly. Therefore one has to rely (for example) on experimental data, for instance measurements of the mole fraction y. An estimate for the true parameters is then obtained by finding a parameter vector matching the collected data, which leads to a least-squares problem constrained by a partial differential equation. However, due to errors in the measurement process the obtained estimate is biased and could be far from the value which describes the physical process most accurately. This bias

has to be quantified and the measurement procedure has to be adapted to mitigate the influence of the perturbed data.

In this manuscript, we consider a general PDE-model based on a parameter-dependent weak formulation with an unknown parameter vector q in an admissible set $Q_{ad} \subset \mathbb{R}^d$ (for instance, $q = (D, E) \in \mathbb{R}^2$ for (1.1)). We refer to section 2.1 for the precise assumptions. The parameter is estimated from point-wise observations of the solution $y = S[q]$ of the PDE-model at points $\{ x_j \}_j^m \subset \Omega_o$, where $\Omega_o \subset \bar{\Omega}$ is a closed set covering the possible observation locations. We choose optimal designs according to criteria based on a linearization of the model equation. To this purpose, we define the associated sensitivities $\{\partial_k S[\hat{q}]\}_{k=1}^n$ of $S[\hat{q}]$ with respect to pertubations of each parameter q_k, $k = 1, \dots, n$ at an initial guess $\hat{q} \in Q_{ad}$, stemming either from prior knowledge or obtained from previous experiments. We note that optimal design approaches based on first-order approximations have been studied for and successfully applied to ordinary differential equations [5], differential-algebraic equations [8], and also partial differential equations [31]. To each measurement location x_j we assign a positive scalar λ_j which is proportional to the quality of the sensor at this location (or, alternatively corresponds to the number of repeated measurements performed with an identical sensor). Associated to the measurement setup is the design measure

$$\boldsymbol{\omega}(x, \lambda) = \sum_{j=1}^{m} \lambda_j \delta_{x_j}, \tag{1.2}$$

given by a weighted sum of Dirac delta functions. To quantify the quality of a given measurement setup ω, we introduce the Fisher information matrix $\mathcal{I}(\omega)$ with entries

$$\mathcal{I}(\omega)_{kl} = \int_{\Omega_o} \partial_k S[\hat{q}](x) \partial_l S[\hat{q}](x) \, \mathrm{d}\omega(x), \quad k, l \in \{1, \dots, n\}. \tag{1.3}$$

Furthermore, by Ψ we denote a scalar quality criterion, which is a positive, smooth, and convex functional acting on the symmetric, positive-definite matrices. Examples for possible choices of Ψ can be found in, e.g., [53, 45]; see also section 3.2. We consider optimal designs given by the solutions to the optimization problem

$$\min_{x_j \in \Omega_o,\, \lambda_j \geq 0,\, j=1,\dots,m} \quad \Psi(\mathcal{I}(\boldsymbol{\omega}(x, \lambda)) + \mathcal{I}_0) + \beta \sum_{j=1}^{m} \lambda_j, \tag{1.4}$$

where $\mathcal{I}_0$ is a nonnegative-definite matrix (e.g., $\mathcal{I}_0 = 0$). It can be interpreted as a priori knowledge on the distribution of the estimator, which may be obtained from previously collected data, for instance in the context of sequential optimal design; cf. [39]. Here, we would choose $\mathcal{I}_0 = \mathcal{I}(\omega_{\text{old}})$ where the design measure ω_{old} describes the previous experiments. Alternatively, we may adopt a Bayesian viewpoint and consider $\mathcal{I}_0$ as the covariance matrix of a Gaussian prior. The last term involving the total amount of measurements and a cost parameter $\beta > 0$ takes into account the overall cost of the measurement process. For other optimal design approaches with sparsity promoting regularization we refer to, e.g., [20, 30, 2]. We emphasize that neither we put any a priori restrictions on the number of measurements nor on the possible locations of the sensors. For instance, we do not restrict the set of candidate locations for the sensors to a finite set.

At first glance, problem (1.4) is a non-convex problem due to the parameterization in terms of the points x_j, and has a combinatorial aspect due to the unknown number of measurements m. However, we can bypass these difficulties by embedding the problem into a more general abstract formulation: introducing the set of positive Borel measures

$M^+(\Omega_o)$ on Ω_o we determine an optimal design measure from

$$\min_{\omega \in M^+(\Omega_o)} \Psi(\mathcal{I}(\omega) + \mathcal{I}_0) + \beta \|\omega\|_{M(\Omega_o)}, \tag{P_β}$$

where $\|\omega\|_{M(\Omega_o)}$ is the canonical total variation norm. While it is clear that (P_β) is a more general formulation than (1.4), it can be shown that it always admits solutions of the form $\omega = \sum_{j=1}^m \lambda_j \delta_{x_j}$ for some $n \leq m \leq n(n+1)/2$, making both problem formulations essentially equivalent; see Section 3.2. We give a brief description of the derivation of (1.4) and its connection to (P_β) in Section 2.

As an alternative to the penalization term $\beta\|\omega\|_{M(\Omega_o)}$ in (P_β) it is possible to consider a fixed budget for the experiment leading to

$$\min_{\omega \in M^+(\Omega_o)} \Psi(\mathcal{I}(\omega) + \mathcal{I}_0) \quad \text{subject to} \quad \|\omega\|_{M(\Omega_o)} \leq K, \tag{P^K}$$

where $K > 0$ denotes the overall maximal cost of the measurements. Under certain conditions on Ψ it can be shown that the inequality constraint in (P^K) is attained for every optimal design; see Proposition 3.8. This relates (P^K) closely to the concept of approximate designs introduced by Kiefer and Wolfowitz in [38] for general linear-regression, where possible experiments are modeled by the probability measures on Ω_o. We refer also to [3, 45, 41, 26, 28] for the analysis of this kind of optimal design formulations. For the adaptation of this approach to parameter estimation in distributed systems we refer to [53, 6]. Both formulations, (P_β) and (P^K), are closely linked (see Section 3.2): On the one hand, in the case of no a priori knowledge on the prior covariance, i.e. for $\mathcal{I}_0 = 0$, the solutions of both problems coincide up to a scalar factor, depending on either K or β. On the other hand, incorporating a priori knowledge, both problem formulations parameterize the same solution manifold. The parameters β and K, respectively, provide some indirect control over the number of measurements, which is the cardinality of the support of the optimal solution, in this case.

This paper is mainly concerned with the analysis of the optimality system for (P_β), its efficient numerical solution and discretization. There exists a large amount of literature on the solution of (P^K) by sequentially adding new Dirac delta functions to a sparse initial design measure. A description and proofs of convergence for several variants of these kind of methods can be found in, e.g., [26, 57] for the special case of $\Psi = \det(\cdot)^{-1}$. These methods correspond to a conditional gradient, or Frank-Wolfe, algorithm, [29], for minimizing the smooth functional $\Psi(\mathcal{I}(\cdot))$ over the ball with radius K in $M^+(\Omega_o)$. Despite the ease of implementation the proposed methods suffer from some serious drawbacks. On the one hand the speed of convergence is slow. Recently, in [13] a sub-linear $\mathcal{O}(1/k)$ rate of convergence for the error in the objective function in terms of the iteration number k was proven by using an equivalent reformulation of (P^K) and results for the classical, finite dimensional conditional gradient algorithm; see, e.g., [36]. Note, that without further assumptions on Ψ than convexity and for example Lipschitz-continuity of its gradient, no better rate than $\mathcal{O}(1/k)$ can be expected in general; see [22, 23].

On the other hand, if only point insertion steps are considered, the support points of the iterates tend to cluster around the optimal ones. To mitigate this effect and accelerate the convergence several modified variants of the sequential point insertion have been proposed. In [48, 4] the authors propose to alternate between point insertion steps and Wolfe's away steps (see [56]) to remove mass from non-optimal points. Heuristically, adjacent support points may be lumped together; see [27]. More recently several papers suggested to combine the addition of a single Dirac-Delta in each iteration with the solution of a finite-dimensional convex optimization problem in each iteration and point moving [13] or vertex exchange

methods [58]. However it appears that there is no rigorous approach to guarantee the convergence of the resulting algorithms towards a finitely supported optimal design on the function space level.

In this paper we present a sequential point insertion algorithm for the (non-smooth) optimal design problem (P_β) and prove convergence towards a sparse minimizer of (P_β) comprising at most $n(n+1)/2$ support points. To this purpose, we adapt the generalized conditional algorithm in measure space presented in [16] for the minimization of a linear-quadratic Tikhonov-regularized problem to our setting. Additionally we incorporate a post-processing step which ensures that the support size of the generated iterates stays uniformly bounded. For further sparsification and a practical acceleration of convergence we propose to alternate between inserting several Dirac delta functions and point removal steps based on the (approximate) solution of finite-dimensional ℓ_1-regularized sub-problems, which are amenable for semi-smooth Newton methods; see, e.g., [54, 40]. We note that strategies based on point moving [16, 13] are difficult to realize for the employed discretization concept introduced in Section 5, since we will employ standard C^0-finite elements, which are not continuously differentiable. A sublinear rate of convergence for the value of the objective function is proven for a wide class of optimality criteria Ψ; see Theorem 4.6. As a comparison, we report on a path-following approach based on a Hilbert space regularization of (P_β); see [21].

Finally, to solve (P_β) or (P^K) one has to compute the state $y = S[q]$ as well as the sensitivities of the state with respect to the parameters $\{\partial_k S[q]\}_{k=1}^n$ for a given $q \in Q_{ad}$. In general, the state and sensitivity PDEs cannot be solved analytically, but only numerically. We present and analyze a discretization scheme for the optimal design problem by replacing the state (and therefore the corresponding sensitivities) by a sequence of finite-element approximations. To discretize the optimal design measure, we adapt the concept of variational discretization from [17, 35], and show the equivalence of a semidiscrete design problem with solutions in $M^+(\Omega_o)$ to a fully discrete one with Dirac delta functions supported only in the grid nodes. Furthermore we prove convergence for a vanishing discretization parameter; see Section 5. To the best of the authors' knowledge this is the first work on a rigorous discretization concept and convergence analysis for an optimal design problem.

The paper is organized as follows: In Section 2 we present the optimal design formulation under consideration. In Section 3 we introduce notation and state basic existence results for solutions to (P_β) as well as first order optimality conditions. In Section 4 the generalized conditional gradient algorithm for the algorithmic solution of (P_β) is proposed and analyzed. Different acceleration/sparsification strategies are presented and a (worst-case) sub-linear convergence rate for the objective functional is proven. Section 5 discusses the approximation of (P_β) by finite element methods. The paper is completed by two numerical examples, a parameter identification problem with three parameters, and a variable parameter example derived from a discretization of a distributed parameter problem; see Section 6. The results serve to illustrate the theoretical results and show the practical efficiency of the proposed algorithms. In particular, we investigate the effect of the described acceleration strategies.

2. From Parameter estimation to optimal design

In this section we derive the convex optimal design formulation (P_β) and establish its connection to the non-convex problem (1.4). Therefore we start by defining a least-squares estimator for the identification of the unknown parameter and the notion of the associated linearised confidence domains.

2.1. **Parameter estimation.** Within the scope of this work we consider the identification of a parameter q entering a weak form $a(\cdot,\cdot)(\cdot)\colon\ Q_{ad} \times \hat{Y} \times Y \to \mathbb{R}$, which can be nonlinear in its first two arguments but is linear in the last one. Here, $Q_{ad} \subset \mathbb{R}^n$, $n \in \mathbb{N}$, denotes a set of admissible parameters, Y denotes a suitable Hilbert space of functions, and $\hat{Y} = \hat{y} + Y$, where the function $\hat{y}$ allows to include non-homogeneous (Dirichlet-type) boundary conditions in the model. For every $q \in Q_{ad}$ a function $y = S[q] \in \hat{Y}$ is called the state corresponding to q if it is a solution to

$$a(q,y)(\varphi) = 0 \quad \forall \varphi \in Y. \tag{2.1}$$

The operator $S\colon Q_{ad} \to \hat{Y}$ mapping a parameter q to the associated state is called the parameter-to-state operator. For instance, one might think of a Sobolev space defined on an open and bounded Lipschitz domain $\Omega \subset \mathbb{R}^d$, $d \in \{1,2,3\}$ and as $a(\cdot,\cdot)(\cdot)$ being the weak formulation of an elliptic partial differential operator.

Remark 1. Concretely, in the case of PDE (1.1), we define

$$a(q,y)(\varphi) = (\nabla y, \nabla\varphi)_{L^2(\Omega)} + (\alpha\nabla y, \varphi)_{L^2(\Omega)} + (D\exp\{-E/(d-y)\}\, y(c-y), \varphi)_{L^2(\Omega)},$$

and $Y = \{\, \varphi \in H^1(\Omega) \mid \varphi|_{\Gamma_{\text{in}}} = 0 \,\}$. In this case the parameter vector is given by $q = (D,E) \in \mathbb{R}^2$.

We make the following general regularity assumption.

Assumption 1. For every $q \in Q_{ad}$ there exists a unique solution $y \in \hat{Y} \cap C(\Omega_o)$ to (2.1). The parameter-to-state mapping S with

$$S\colon Q_{ad} \to C(\Omega_o) \quad \text{with} \quad q \mapsto S[q] = y,$$

is continuously differentiable in a neighborhood of Q_{ad} in $\mathbb{R}^n$. We denote by $\partial_k S[q] \in C(\Omega_o)$ the directional derivative of S in the direction of the k-th unit vector and by $\partial S[q] \in C(\Omega_o, \mathbb{R}^n)$ the vector of partial derivatives.

We emphasize that under suitable differentiability assumptions on the form $a(\cdot,\cdot)$ and Assumption 1 the k-th partial derivative $\delta y_k = \partial_k S[q] \in Y \cap C(\Omega_o)$, $k = 1,\dots,n$ is the unique solution of the sensitivity equation

$$a'_y(q,y)(\delta y_k, \varphi) = -a'_{q_k}(q,y)(\varphi), \quad \forall \varphi \in Y, \tag{2.2}$$

where $y = S[q]$ and a'_y and a'_{q_k} denote the partial derivatives of the form a with respect to the state and the k-th parameter; see, e.g., [55, 52].

In the following the exact value of the parameter vector $q \in \mathbb{R}^n$ appearing in (2.1) is denoted by q^*. While, for the purposes of analysis we can assume this value to be known, it will be replaced with an appropriate a priori guess in practice. To estimate the parameter q we consider measurement data y_d collected at a set of m disjoint sensor locations $\{x_j\}_{j=1}^m \subset \Omega_o$, where $\Omega_o \subset \bar{\Omega}$ is a closed set. To take measurement errors into account we assume that the data $y_d^j \approx S[q^*](x_j)$ is additively perturbed by independently unit normally distributed noise; see, e.g., [7]. Here $S[q^*](x_j)$ denotes the response of the model to the exact parameter values. Taking into account that multiple measurements can be performed at the same location, we obtain that

$$y_d^j = S[q^*](x_j) + \epsilon_j,\ \epsilon_j \sim \mathcal{N}(0, 1/\lambda_j),\ \operatorname{Cov}(\epsilon_j, \epsilon_i) = 0,$$

for all $i,j = 1,\dots,m$, and $j \neq i$, where $\lambda_j \in \mathbb{N} \setminus \{\,0\,\}$ denotes the number of measurements taken at the j-th location. More generally, we assume that λ_j can be chosen arbitrarily in $\mathbb{R}_+ \setminus \{\,0\,\}$ in the following. In this case the measurement weights $\lambda_j > 0$ should be

interpreted as diligence factors giving information on how carefully the data should be collected at the corresponding measurement point.

To emphasize that the data y_d is a random variable conditional on the measurement errors we will write $y_d(\varepsilon)$ in the following and define the least squares functional

$$J(q,\varepsilon) = \frac{1}{2}\sum_{j=1}^{m} \lambda_j (S[q](x_j) - y_d^j(\varepsilon))^2 \tag{2.3}$$

as well as the possibly multi-valued least squares estimator

$$\tilde{q}\colon \mathbb{R}^m \to \mathcal{P}(\mathbb{R}^n),\ \tilde{q}(\varepsilon) = \operatorname*{arg\,min}_{q\in Q_{ad}} J(q,\varepsilon), \tag{2.4}$$

where $\mathcal{P}(\mathbb{R}^n)$ denotes the power set of $\mathbb{R}^n$. Note that this estimator is the usual Maximum-Likelihood estimator using the assumption on the distribution measurement errors $\varepsilon_j \sim \mathcal{N}(0, 1/\lambda_j)$.

2.2. **Optimal design.** Since the measurement errors are modelled as random variables, the uncertainty in the data is also propagated to the estimator. This means that $\tilde{q}$ should be interpreted as a random vector. To quantify the bias in the estimation and to assess the quality of computed realizations of the estimator, one considers the non-linear confidence domain of $\tilde{q}$ defined as

$$D(\tilde{q},\alpha)(\epsilon) = \left\{ p \in Q_{ad} \mid J(p,\epsilon) - \min_{q\in Q_{ad}} J(q,\epsilon) \le \gamma_n^2(\alpha) \right\}, \tag{2.5}$$

where $\gamma_n^2(\alpha)$ denotes the $(1-\alpha)$-quantile of the χ^2-distribution with n degrees of freedom; see, e.g., [11, 9]. We emphasize that the confidence domain is a function of the measurement errors and therefore a random variable whose realizations are subsets of the parameter space. In this context, the confidence level $\alpha \in (0,1)$ gives the probability that a certain realization of $D(\tilde{q}(\epsilon),\alpha)(\epsilon)$ contains the true parameter vector q^*.

Consequently, a good performance indicator for the estimator $\tilde{q}$ is given by the size of its associated confidence domains. The smaller their size, the closer realizations of $\tilde{q}$ will be to q^* with a high probability. Given a realization $D(\bar{q},\alpha)(\bar{\epsilon})$ of the non-linear confidence domain, its size only depends on the position and the number of the measurements. To obtain a more reliable estimate for the parameter vector, the experiment, e.g. the total number of measurements carried out, their positions x_j, and the measurement weights λ_j should be chosen a priori in such a way that confidence domains of the resulting estimator are small. However, for general models and parameter-to-state mappings S the estimator $\tilde{q}$ cannot be given in closed form. Therefore it is generally not possible to provide an exact expression for $D(\tilde{q},\alpha)$.

To circumvent this problem we follow the approach proposed in, e.g., [44, 28] and consider a linearisation of the original model around an a priori guess $\hat{q}$ of q^* which can stem from historical data or previous experiments. In the following, $\epsilon \in \mathbb{R}^m$ denotes an arbitrary vector of measurement errors, and $x \in \mathbb{R}^{d\times m}$, $x = (x_1,\dots,x_m)$, with $x_j \in \mathbb{R}^d$, $j = 1,\dots,m$, stands for the measurement locations. For abbreviation we write $S[\hat{q}](x) \in \mathbb{R}^m$ for the vector of observations with $S[\hat{q}](x)_j = S[\hat{q}](x_j)$, $j = 1,\dots,m$. Moreover the matrices $X \in \mathbb{R}^{m\times n}$ and $\Sigma^{-1} \in \mathbb{R}^{m\times m}$ are defined as

$$X_{jk} = \partial_k S[\hat{q}](x_j), \quad \Sigma^{-1}_{ij} = \delta_{ij}\lambda_i, \quad i,j = 1,\dots,m,\ k = 1,\dots,n,$$

and are assumed to have full rank. We arrive at the linearised least-squares functional

$$J_{\mathrm{lin}}(q,\epsilon) = \frac{1}{2}\sum_{j=1}^{m} \lambda_j (S[\hat{q}](x_j) + \partial S[\hat{q}](x_j)^\top (q-\hat{q}) - y_d^j(\epsilon))^2,$$

which can be equivalently written as

$$J_{\mathrm{lin}}(q,\epsilon) = \frac{1}{2}\|X(q-\hat{q}) + S[\hat{q}](x) - y_d(\epsilon)\|_{\Sigma^{-1}}^2,$$

where $\|v\|_{\Sigma^{-1}} = v^\top \Sigma^{-1} v$ for $v \in \mathbb{R}^n$. In contrast to the estimator $\tilde{q}$ (2.4), the associated linearised estimator

$$\tilde{q}_{\mathrm{lin}} \colon \mathbb{R}^m \to \mathbb{R}^n, \quad \tilde{q}_{\mathrm{lin}}(\epsilon) = \operatorname*{arg\,min}_{q\in\mathbb{R}^n} J_{\mathrm{lin}}(q,\epsilon), \tag{2.6}$$

is single-valued and its realizations can be calculated explicitly (see, e.g., [51]), as

$$\tilde{q}_{\mathrm{lin}}(\epsilon) = \hat{q} + (X^\top \Sigma^{-1} X)^{-1} X^\top \Sigma^{-1} \left(y_d(\epsilon) - S[\hat{q}](x)\right). \tag{2.7}$$

Due to the assumptions on the noise ϵ the estimator $\tilde{q}_{\mathrm{lin}}$ is a Gaussian random variable with $\tilde{q}_{\mathrm{lin}} \sim \mathcal{N}(\tilde{q}_{\mathrm{lin}}(0), (X^\top \Sigma^{-1} X)^{-1})$. The associated realizations of its confidence domain (see, e.g., [11]) are thus given by

$$D(\tilde{q}_{\mathrm{lin}},\alpha)(\epsilon) = \left\{ q \in \mathbb{R}^n \mid q = \tilde{q}_{\mathrm{lin}} + (X^\top \Sigma^{-1} X)^{-1} X^\top \Sigma^{-1/2} \delta\epsilon,\ \|\delta\epsilon\|_2 \le \gamma_n(\alpha) \right\}, \tag{2.8}$$

where $\|\cdot\|_2$ denotes the Euclidean norm. We point out that the linearised confidence domains are ellipsoids in the parameter space centered around $\tilde{q}_{\mathrm{lin}}$. Their half axes are given by the eigenvectors of the Fisher-information matrix $\mathcal{I} = X^\top \Sigma^{-1} X$ with lengths proportional to the associated eigenvalues. Their sizes depend only on the a priori guess $\hat{q}$ and the setup of the experiment, i.e. the position and total number of measurements, but not on the concrete realization of the measurement noise. Consequently we can improve the estimator by minimizing the linearised confidence domains as a function of the measurement setup, which leads to (1.4).

To establish the connection to the sparse optimal design approach we observe that the entries of the Fisher-information matrix can be written alternatively as

$$(X^\top \Sigma^{-1} X)_{kl} = \sum_{j=1}^{m} \partial_k S[\hat{q}](x_j) \partial_l S[\hat{q}](x_j) \lambda_j = \int_{\Omega_o} \partial_k S[\hat{q}] \partial_l S[\hat{q}] \,\mathrm{d}\omega = \mathcal{I}(\omega)_{kl}, \tag{2.9}$$

with the design measure $\omega = \sum_{j=1}^m \lambda_j \delta_{x_j}$. Furthermore we note that for such a design measure there holds $\|\omega\|_{M(\Omega_o)} = \sum_{j=1}^m \lambda_j$. Consequently, for some design criterion Ψ and prior knowledge $\mathcal{I}_0$, the optimal design problem (1.4) can be equivalently expressed as

$$\min_{\omega \in \mathrm{cone}\{\,\delta_x \mid x\in\Omega_o\,\}} \quad \Psi(\mathcal{I}(\omega) + \mathcal{I}_0) + \beta\|\omega\|_{M(\Omega_o)}, \tag{2.10}$$

where we minimize the objective functional over all non-negative linear combinations of Dirac delta functions corresponding to points in the observational domain. A priori it is however unclear if this reformulation admits an optimal solution, since the admissible set is not closed in the weak* topology on $M(\Omega_o)$. For a rigorous analysis one therefore has to pass to the closure $\overline{\mathrm{cone}\{\,\delta_x \mid x\in\Omega_o\,\}}^* = M^+(\Omega_o)$. As (2.9) suggests, the definition of $\mathcal{I}$ can be extended to the set of positive regular Borel measures $M^+(\Omega_o)$, resulting in the more general problem formulation (P_β).

3. Analysis of the optimal design problem

3.1. **Notation and assumptions.** In the following we fix the general notation for the remainder of the paper. We consider an observation set Ω_o in which we allow the collection of measurements. It is assumed to be a closed subset of $\bar{\Omega}$, which is the closure of the bounded spatial domain $\Omega \subset \mathbb{R}^d$. On Ω_o we define the space of regular Borel measures $M(\Omega_o)$ as the topological dual of $C(\Omega_o)$, the space of continuous and bounded functions (see, e.g., [25]), with associated duality pairing $\langle \cdot, \cdot \rangle$. The norm on $M(\Omega_o)$ is given by

$$\|\omega\|_{M(\Omega_o)} = \sup_{y \in C(\Omega_o),\, \|y\|_{C(\Omega_o)} \leq 1} \langle y, \omega \rangle,$$

where $\|\cdot\|_{C(\Omega_o)}$ is the supremum norm on $C(\Omega_o)$. By $M^+(\Omega_o)$ we refer to the set of positive Borel measures on Ω_o (see, e.g., [47, Def. 1.18]),

$$M^+(\Omega_o) = \{\, \omega \in M(\Omega_o) \mid \langle y, \omega \rangle \geq 0,\ \forall y \in C(\Omega_o)\ y \geq 0 \,\},$$

with convex indicator function $I_{\omega \geq 0}$. Given a measure $\omega \in \Omega_o$ its support is defined as usual by

$$\operatorname{supp} \omega = \Omega_o \backslash \left\{ \bigcup B \in \mathcal{B}(\Omega_o) \mid B \text{ open}, \omega(B) = 0 \right\}.$$

Note that the support is a closed set. A sequence $\{\omega_k\} \subset M(\Omega_o)$ is called convergent with respect to the weak*-topology with limit $\omega \in M(\Omega_o)$ if $\langle y, \omega_k \rangle \to \langle y, \omega \rangle$ for $k \to \infty$ for all $y \in C(\Omega_o)$ indicated by $\omega_k \overset{*}{\rightharpoonup} \omega$. Additionally we define the usual spaces of integrable and square integrable functions $L^1(\Omega_o)$ and $L^2(\Omega_o)$, respectively, as well as the usual Sobolev space $H_0^1(\Omega_o)$ with their usual (semi)norm and inner product; see, e.g., [1]. Furthermore we denote by $\mathrm{Sym}(n)$, $\mathrm{NND}(n)$, and $\mathrm{PD}(n)$ the sets of symmetric, symmetric non-negative definite, and symmetric positive definite matrices, respectively. On $\mathrm{Sym}(n)$ we consider the inner product $(A, B)_{\mathrm{Sym}(n)} = \mathrm{Tr}(AB^\top)$ for $A, B \in \mathrm{Sym}(n)$, where Tr denotes the trace, and the Löwner partial order

$$0 \leq_L A \ \Leftrightarrow\ A \text{ is positive semidefinite.}$$

Last, for $\phi \colon M(\Omega_o) \to \mathbb{R} \cup \{\infty\}$ and a convex set $M \subset M(\Omega_o)$ we define the domain of ϕ over M as

$$\operatorname{dom}_M \phi = \{\, \omega \in M \mid \phi(\omega) < \infty \,\},$$

where the index is omitted when $M = M(\Omega_o)$.

We consider design criteria of the form $\Psi(\cdot + \mathcal{I}_0)$, where $\mathcal{I}_0 \in \mathrm{NND}(n)$ (e.g. $\mathcal{I}_0 = 0$) incorporates prior knowledge, as described in the introduction. Concerning the function Ψ the following assumptions are made.

Assumption 2. The function $\Psi \colon \mathrm{Sym}(n) \to \mathbb{R} \cup \{+\infty\}$ satisfies:

- **A1** There holds $\operatorname{dom} \Psi = \mathrm{PD}(n)$.
- **A2** Ψ is continuously differentiable for every $N \in \mathrm{PD}(n)$.
- **A3** Ψ is non-negative on $\mathrm{NND}(n)$.
- **A4** Ψ is lower semi-continuous and convex on NND.
- **A5** Ψ is monotone with respect to the Löwner ordering on $\mathrm{NND}(n)$, i.e. there holds

$$N_1 \leq_L N_2 \Rightarrow \Psi(N_1) \geq \Psi(N_2) \quad \forall N_1,\ N_2 \in \mathrm{NND}(n).$$

While Assumptions (**A1**) to (**A4**) are important for the existence of optimal designs and the derivation of first order optimality conditions, Assumption (**A5**) is related to the size

of the linearised confidential domains (2.8). Given two design measures $\omega_1, \omega_2 \in M^+(\Omega_o)$ with $\mathcal{I}(\omega_1), \mathcal{I}(\omega_1) \in \mathrm{PD}(n)$ there holds

$$\mathcal{I}(\omega_1) \leq_L \mathcal{I}(\omega_2) \Leftrightarrow \mathcal{I}(\omega_2)^{-1} \leq_L \mathcal{I}(\omega_1)^{-1},$$

where the latter statement implies

$$\mathcal{E}_2 = \{\, \delta q \in \mathbb{R}^n \mid \delta q^\top \mathcal{I}(\omega_2)^{-1} \delta q \leq r \,\} \subset \mathcal{E}_1 = \{\, \delta q \in \mathbb{R}^n \mid \delta q^\top \mathcal{I}(\omega_1)^{-1} \delta q \leq r \,\}$$

for any $r > 0$. This ensures that Ψ is indeed a suitable criterion for the size of the linearised confidence ellipsoids (2.8). For a similar set of conditions; see [53, p. 41]. The given assumptions can be verified for a large class of classical optimality criteria, among them the A and D criterion

$$\Psi_A(N) = \begin{cases} \mathrm{Tr}(N^{-1}), & N \in \mathrm{PD}(n), \\ \infty, & \text{else}, \end{cases} \qquad \Psi_D(N) = \begin{cases} \det(N^{-1}), & N \in \mathrm{PD}(n), \\ \infty, & \text{else}, \end{cases}$$

corresponding to the combined length of the half axis and the volume of the confidence ellipsoids. Additionally, one may also use weighted versions of the design criteria: for instance $\Psi_A^w(N) = \mathrm{Tr}(WN^{-1}W)$ allows to put special emphasis on particular parameters by virtue of the weight matrix $W \in \mathrm{NND}(n)$. However, we emphasize that the results presented in this paper cannot be applied to other non-differentiable popular criteria such as the E criterion defined by

$$\Psi_E(N) = \begin{cases} \max_i \{\lambda_i(N^{-1})\}, & N \in \mathrm{PD}(n), \\ \infty, & \text{else}. \end{cases}$$

describing the length of the longest half axis and the length of the longest side of the smallest box containing the confidence ellipsoid. In this case, one can for instance resort to smooth approximations of the design criteria.

3.2. **Existence of optimal solutions to (P_β) and optimality conditions.** In this section we prove the existence of solutions as well as first order necessary and sufficient optimality conditions for the optimal design problem (P_β). Additionally, results on the sparsity pattern of optimal designs are derived. First, we introduce the linear and continuous Fisher-operator $\mathcal{I}$ by

$$\mathcal{I}\colon M(\Omega_o) \to \mathrm{Sym}(n), \quad \text{with} \quad \mathcal{I}(\omega)_{i,j} = \langle \partial_i S[\hat{q}] \partial_j S[\hat{q}], \omega \rangle \quad \forall i,j \in \{\,1,\dots,n\,\}.$$

It is readily verified that it is the Banach space adjoint of the operator

$$\mathcal{I}^*\colon \mathrm{Sym}(n) \to C(\Omega_o), \quad \text{with} \quad \mathcal{I}^*(A) = \varphi_A,$$

where $\varphi_A \in C(\Omega_o)$ is the continuous function given for $A \in \mathrm{Sym}(n)$ by

$$\varphi_A(x) = \mathrm{Tr}\left(\partial S[\hat{q}](x) \partial S[\hat{q}](x)^\top A\right) = \partial S[\hat{q}](x)^\top A\, \partial S[\hat{q}](x) \quad \forall x \in \Omega_o. \tag{3.1}$$

Now, we formulate the reduced design problem (P_β) as

$$\min_{\omega \in M^+(\Omega_o)} F(\omega) = \psi(\omega) + \beta \|\omega\|_{M(\Omega_o)},$$

where $\psi(\omega) = \Psi(\mathcal{I}(\omega) + \mathcal{I}_0)$. In the following proposition we collect some properties of the reduced functional.

Proposition 3.1. *Let Assumptions (**A1**)–(**A5**) be fulfilled and let $\mathcal{I}_0 \in \mathrm{NND}(n)$ be given. The operator $\mathcal{I}$ and the functional ψ satisfy:*

1. *For every $\omega \in M^+(\Omega_o)$ there holds $\mathcal{I}(\omega) \in \mathrm{NND}(n)$.*
2. *There holds $\mathrm{dom}_{M^+(\Omega_o)} \psi = \{\, \omega \in M^+(\Omega_o) \mid \mathcal{I}(\omega) + \mathcal{I}_0 \in \mathrm{PD}(n) \,\}$.*

3. *ψ is differentiable with derivative $\psi'(\omega) = \mathcal{I}^*\left(\Psi'(\mathcal{I}(\omega)+\mathcal{I}_0)\right) \in C(\Omega_o)$ for every $\omega \in \operatorname{dom}_{M^+(\Omega_o)}\psi$. The derivative can be identified with the continuous function*

$$\left[\psi'(\omega)\right](x) = \partial S[q](x)^\top \Psi'(\mathcal{I}(\omega)+\mathcal{I}_0)\,\partial S[q](x) \quad \forall x \in \Omega_o. \tag{3.2}$$

Moreover the gradient $\psi'\colon \operatorname{dom}_{M^+(\Omega_o)}\psi \to C(\Omega_o)$ is weak-to-strong continuous.*

4. *ψ is non-negative on $\operatorname{dom}_{M^+(\Omega_o)}\psi$.*
5. *ψ is weak* lower semi-continuous and convex on $M^+(\Omega_o)$.*
6. *ψ is monotone in the sense that*

$$\mathcal{I}(\omega_1) \leq_L \mathcal{I}(\omega_2) \Rightarrow \psi(\omega_1) \geq \psi(\omega_2) \quad \forall \omega_1,\ \omega_2 \in M^+(\Omega_o).$$

Proof. To prove the first claim we observe that there holds

$$z^\top \mathcal{I}(\omega) z = \langle (\partial S[\hat{q}]^\top z)^2, \omega\rangle \geq 0 \quad \forall z \in \mathbb{R}^n \tag{3.3}$$

for an arbitrary $\omega \in M^+(\Omega_o)$, thus $\mathcal{I}(\omega) \in \mathrm{NND}(n)$. Statement 2. follows directly with (**A1**). For $\omega \in \operatorname{dom}_{M^+(\Omega_o)}\psi$ the differentiability of ψ follows from assumption (**A2**) using the chain rule. We obtain the derivative $\psi'(\omega) \in M(\Omega_o)^*$ characterized by

$$\langle \psi'(\omega), \delta\omega\rangle_{M^*,M} = \operatorname{Tr}(\Psi'(\mathcal{I}(\omega)+\mathcal{I}_0)\,\mathcal{I}(\delta\omega)) = \langle \mathcal{I}^*\left(\Psi'(\mathcal{I}(\omega)+\mathcal{I}_0)\right), \delta\omega\rangle_{M^*,M},$$

for every $\delta\omega \in M(\Omega_o)$, where $\langle\cdot,\cdot\rangle_{M^*,M}$ denotes the duality pairing between $M(\Omega_o)$ and its topological dual space. Using the adjoint expression for $\mathcal{I}$ given in (3.1) we can identify $\psi'(\omega)$ with the continuous function (3.2). Additionally, we directly see that the mapping $\psi'\colon \operatorname{dom}_{M^+(\Omega_o)}\psi \to C(\Omega_o)$, $\omega \mapsto \psi'(\omega)$ is weak*-to-strong continuous, using the continuity of Ψ'. Statements 4., 5., and 6. can be derived directly from Assumptions (**A2**), (**A4**), and (**A5**) using $\mathcal{I}(\omega_k) \to \mathcal{I}(\omega)$ for every sequence $\{\omega_k\}_{k\in\mathbb{N}} \subset M^+(\Omega_o)$ with weak* limit ω. □

Proposition 3.2. *Assume that $\operatorname{dom}_{M^+(\Omega_o)}\psi \neq \emptyset$ and $\beta > 0$. Then there exists at least one optimal solution $\bar{\omega}_\beta$ to (P_β). Moreover the set of optimal solutions is bounded. If Ψ is strictly convex on $\mathrm{PD}(n)$ then the optimal Fisher-information matrix $\mathcal{I}(\bar{\omega}_\beta)$ is unique.*

Proof. The proof follows standard arguments, using the direct method in variational calculus, using the estimate $\|\omega\|_{M(\Omega_o)} \leq F(\omega)/\beta$, the sequential version of the Banach-Alaoglu theorem, and the facts that F is proper and weak* lower-semicontinuous. The boundedness of the set of optimal solutions is another direct consequence. Additionally, uniqueness of the otimal Fisher information matrix can be deduced from strict convexity of Ψ by a direct contradiction arguments. □

Next we give conditions for the domain of ψ to be non-empty.

Proposition 3.3. *Assume that $\beta > 0$ and*

$$\mathbb{R}^n = \operatorname{span}\left(\operatorname{Ran}\mathcal{I}_0 \cup \{\,\partial S[\hat{q}](x) \mid x \in \Omega_o\,\}\right).$$

Then there exists at least one optimal solution of (P_β). Furthermore, every $\omega \in \operatorname{dom}_{M^+(\Omega_o)}\psi$ consists of at least $n_0 = n - \operatorname{rank}\mathcal{I}_0$ support points.

Proof. According to Proposition 3.2 we have to show that there exists $\omega \in \operatorname{dom}_{M^+(\Omega_o)}\psi$. By assumption we can choose a set of $n - \operatorname{rank}\mathcal{I}_0$ distinct points $x_j \in \Omega_o$ such that

$$\mathbb{R}^n = \operatorname{span}\left(\operatorname{Ran}\mathcal{I}_0 \cup \{\,\partial S[\hat{q}](x_j) \mid j = 1,\dots,n-\operatorname{rank}\mathcal{I}_0\}\right).$$

Consequently, setting $\omega = \sum_{j=1}^{n_0}\delta_{x_j} \in M^+(\Omega_o)$, we obtain

$$\mathcal{I}(\omega)+\mathcal{I}_0 = \sum_{j=1}^{n_0} \partial S[\hat{q}](x_j)\partial S[\hat{q}](x_j)^\top + \mathcal{I}_0 \in \mathrm{PD}(n),$$

by straightforward arguments. For the last statement we simply observe that for a measure ω with less than $n_0 = n - \operatorname{rank}\mathcal{I}_0$ support points, the associated information matrix $\mathcal{I}(\omega) + \mathcal{I}_0$ has a non-trivial kernel. □

By standard results from convex analysis the following necessary and sufficient optimality conditions can be obtained.

Proposition 3.4. *Let $\bar\omega_\beta \in \operatorname{dom}_{M^+(\Omega_o)} \psi$ be given. Then $\bar\omega_\beta$ is an optimal solution to (P_β) if and only if holds:*

$$\langle -\psi'(\bar\omega_\beta), \omega - \bar\omega_\beta\rangle + \beta\|\bar\omega_\beta\|_{M(\Omega_o)} \le \beta\|\omega\|_{M(\Omega_o)} \quad \forall \omega \in M^+(\Omega_o). \tag{3.4}$$

Proof. Since F is convex, a given $\bar\omega_\beta$ is optimal if and only if

$$0 \in \partial\left(F(\bar\omega_\beta) + I_{\omega\ge 0}(\bar\omega_\beta)\right),$$

where the expression on the right denotes the subdifferential of $F + I_{\omega\ge0}$ at $\bar\omega_\beta$ in $M(\Omega_o)^*$. Since the total variation norm and the indicator function of $M^+(\Omega_o)$ are continuous at $\bar\omega_\beta$ and ψ is differentiable on its domain there holds

$$0 \in \partial F(\bar\omega_\beta) = \psi'(\bar\omega_\beta) + \partial(\beta\|\bar\omega_\beta\|_{M(\Omega_o)} + I_{\omega\ge0}(\bar\omega_\beta),$$

which is equivalent to (3.4). □

Since the norm as well as the indicator function are positively homogeneous, their subdifferentials can be characterized further. This yields an equivalent characterization of optimality relating the support points of an optimal design to the set of minimizers of the gradient of ψ in the optimum.

Lemma 3.5. *Let $\bar\omega_\beta$ be an optimal solution to (P_β). Condition* (3.4) *is equivalent to*

$$-\psi'(\bar\omega_\beta) \le \beta, \quad \operatorname{supp}\bar\omega_\beta \subset \left\{x \in \Omega_o \mid \psi'(\bar\omega_\beta)(x) = -\beta\right\}. \tag{3.5}$$

Proof. Assume that $\bar\omega_\beta$ satisfies (3.5). Then for an arbitrary measure $\omega \in M^+(\Omega_o)$ there holds

$$-\langle\psi'(\bar\omega_\beta), \omega - \bar\omega_\beta\rangle + \beta\|\bar\omega_\beta\|_{M(\Omega_o)} = -\langle\psi'(\bar\omega_\beta), \omega\rangle \le \beta\|\omega\|_{M(\Omega_o)},$$

implying (3.4). Conversely, assume that $\bar\omega_\beta$ fulfills (3.4). Testing (3.4) with $\omega = 0$, $\omega = 2\bar\omega_\beta$, and $\omega = \delta_x$ for every $x \in \Omega_o$ respectively, we obtain

$$\begin{aligned} -\langle\psi'(\bar\omega_\beta), \bar\omega_\beta\rangle &\ge \beta\|\bar\omega_\beta\|_{M(\Omega_o)},\\ -\langle\psi'(\bar\omega_\beta), \bar\omega_\beta\rangle &\le \beta\|\bar\omega_\beta\|_{M(\Omega_o)},\\ -\psi'(\bar\omega_\beta)(x) + \langle\psi'(\bar\omega_\beta), \bar\omega_\beta\rangle + \beta\|\bar\omega_\beta\|_{M(\Omega_o)} &\le \beta \quad \forall x \in \Omega_o. \end{aligned}$$

From this we deduce

$$\langle -\psi'(\bar\omega_\beta) - \beta, \bar\omega_\beta\rangle = 0 \quad \text{and} \quad -\psi'(\bar\omega_\beta)(x) \le \beta \quad \forall x \in \Omega_o.$$

The condition on the support of $\bar\omega_\beta$ in (3.5) follows with similar arguments as in [16, Proposition 3]: Let an arbitrary $x \in \Omega_o$ with $-\psi'(\bar\omega_\beta)(x) < \beta$ be given. Due to the continuity of $\psi'(\bar\omega_\beta)$ there exists $\delta > 0$ with $-\psi'(\bar\omega_\beta) < -\beta$ on $B_\delta(x) \subset \Omega_o$. For an arbitrary nonnegative $y \in C(B_\delta(x))$ there exists $t > 0$ such that $\psi'(\bar\omega_\beta) - ty + \beta \ge 0$. From this we conclude

$$0 \le \langle\psi'(\bar\omega_\beta) - ty - \beta, \bar\omega_\beta\rangle = -\langle ty, \bar\omega_\beta\rangle \le 0$$

due to the positivity of y and $\bar\omega_\beta$. Therefore $\bar\omega|_{B_\delta(x)} = 0$ and $B_\delta(x) \subset \Omega_o \setminus \operatorname{supp}\bar\omega$. □

Remark 2. For (P^K) a similar optimality condition can be derived by the same techniques. A measure $\bar{\omega}^K \in \operatorname{dom}_{M^+(\Omega_o)} \psi$ is an optimal solution of (P^K) if and only if

$$\operatorname{supp} \bar{\omega}^K \subset \left\{ x \in \Omega_o \;\middle|\; \psi'(\bar{\omega}^K)(x) = \operatorname*{arg\,min}_{x \in \Omega_o} \psi'(\bar{\omega}^K)(x) \right\},$$

where the condition on the support of $\bar{\omega}^K$ is equivalent to

$$-\langle \psi'(\bar{\omega}^K), \bar{\omega}^K \rangle + \operatorname*{arg\,min}_{x \in \Omega_o} \psi'(\bar{\omega}^K)(x) \|\bar{\omega}^K\|_{M(\Omega_o)} = 0,$$

yielding the well-known Kiefer-Wolfowitz equivalence theorem; see [38, 37] and [53, Theorem 3.2].

Since the Fisher-operator $\mathcal{I}$ is a finite rank operator, uniqueness of the optimal solution is usually not guaranteed. However, the existence of at least one solution with the practically desired sparsity structure is addressed in the following theorem.

Theorem 3.6. *Let $\omega \in M^+(\Omega_o)$ be given. Then there exists $\tilde{\omega} \in M^+(\Omega_o)$ with*

$$\mathcal{I}(\omega) = \mathcal{I}(\tilde{\omega}), \quad \|\tilde{\omega}\|_{M(\Omega_o)} \leq \|\omega\|_{M(\Omega_o)}, \quad \#\operatorname{supp} \tilde{\omega} \leq n(n+1)/2.$$

Additionally, if there exists an optimal solution to (P_β), then there exists an optimal solution $\bar{\omega}_\beta$ with $\#\operatorname{supp} \bar{\omega}_\beta \leq n(n+1)/2$.

Proof. The proof is based on a refined version of Caratheodory's theorem, [50], but will be omitted here. For details we refer to the proof of [43, Proposition B.5]. □

The proof of Theorem 3.6 leads to an implementable sparsifying procedure which, given an arbitrary finitely supported positive measure, finds a sparse measure choosing a subset of at most $n(n+1)/2$ support points and yielding the same information matrix. The procedure is summarized in Algorithm 1.

Proposition 3.7. *Let $\omega = \sum_{i=1}^m \lambda_i \delta_{x_i}$ be given and assume that $\{\mathcal{I}(\delta_{x_i})\}_{i=1}^m$ is linearly dependent. Denote by $\omega_{\text{new}} = \sum_{\{\, i \,|\, \lambda_{\text{new},i} > 0 \,\}} \lambda_{\text{new},i} \delta_{x_i}$ the measure that is obtained after one execution of the loop in Algorithm 1. Then there holds*

$$F(\omega_{\text{new}}) \leq F(\omega), \quad \#\operatorname{supp} \omega_{\text{new}} \leq \#\operatorname{supp} \omega - 1.$$

Proof. See [43, Corollary 6.2] and [43, Proposition B.5] □

Algorithm 1 Support-point removal

1. Let $\omega = \sum_{i=1}^m \lambda_i \delta_{x_i}$ be given.

while $\{\mathcal{I}(\delta_{x_i})\}_{i=1}^m$ linearly dependent **do**

2. Find $0 \neq \bar{\lambda}$ with $0 = \sum_{i=1}^m \bar{\lambda}_i \mathcal{I}(\delta_{x_i})$.
3. Set $\mu = \max_i \{\, \bar{\lambda}_i / \lambda_i \,\}$, $\lambda_{\text{new},i} = \lambda_i - \bar{\lambda}_i / \mu$.
4. Update $\omega_{\text{new}} = \sum_{\{\, i \,|\, \lambda_{\text{new},i} > 0 \,\}} \lambda_{\text{new},i} \delta_{x_i}$.

end while

In the last part of this section we will further discuss structural properties of solutions to (P_β), mainly focusing on their connection to (P^K) and their behaviour for $\beta \to \infty$.

Proposition 3.8. *The problems (P^K) and (P_β) are equivalent in the following sense: Given, for fixed $K > 0$, a solution $\bar{\omega}^K$ to (P^K), there exists a $\beta \geq 0$, such that $\bar{\omega}^K$ is an optimal solution to (P_β) and vice versa.*

Furthermore, assuming that Ψ is strictly monotone with respect to the Löwner ordering in the sense that

$$N_2 - N_1 \in \mathrm{PD}(n) \Rightarrow \Psi(N_1) > \Psi(N_2), \quad N_1, N_2 \in \mathrm{PD}(n),$$

we additionally obtain the following:

- *We have $\|\bar{\omega}^K\|_{M(\Omega_o)} = K$ for each optimal solution $\bar{\omega}^K$ to (P^K).*
- *There exists a function*

$$\beta \colon \mathbb{R}_+ \setminus \{0\} \to \mathbb{R}_+ \setminus \{0\}, \quad K \mapsto \beta(K),$$

such that each optimal solution $\bar{\omega}^K$ to (P^K) is a minimizer of $(P_{\beta(K)})$.

Proof. Fix an arbitrary $K > 0$. By well established results from convex analysis (see, e.g., [12, Proposition 2.153]) the norm-constrained problem (P^K) is calm. Define the Lagrangian L as

$$L \colon M^+(\Omega_o) \times \mathbb{R}_+ \to \mathbb{R}_+ \quad L(\omega, \beta) = \psi(\omega) + \beta(\|\omega\|_{M(\Omega_o)} - K).$$

A given measure $\bar{\omega}^K \in M^+(\Omega_o)$ is optimal for (P^K) if and only if there exists a Lagrange multiplier $\beta \geq 0$ with

$$\bar{\omega}^K \in \operatorname*{arg\,min}_{\omega \in M^+(\Omega_o)} L(\omega, \beta), \quad \beta(\|\bar{\omega}^K\|_{M(\Omega_o)} - K) = 0. \tag{3.6}$$

The set of Lagrange multipliers is independent of the choice of the optimizer $\bar{\omega}^K$, i.e. given two arbitrary optimal solutions $\bar{\omega}_1^K, \bar{\omega}_2^K \in M^+(\Omega_o)$ to (P^K) and $\beta \geq 0$ such that the pair $(\bar{\omega}_1^K, \beta)$ fulfills (3.6), then so does $(\bar{\omega}_2^K, \beta)$. For a proof we refer to, e.g., [12, Theorem 3.4]. This proves the first statement.

Assume that Ψ is strictly monotone. Let $\bar{\omega}^K$ be an arbitrary optimal solution to (P^K) with $\|\bar{\omega}^K\|_{M(\Omega_o)} < K$. Using the strict monotonicity of Ψ we deduce that $\bar{\omega}^K \neq 0$. Defining $\tilde{\omega} = (K/\|\bar{\omega}^K\|_{M(\Omega_o)})\bar{\omega}^K$ there holds $\psi(\tilde{\omega}) < \psi(\bar{\omega}^K)$ since $(K/\|\bar{\omega}^K\|_{M(\Omega_o)}) > 1$. This gives a contradiction and $\|\bar{\omega}^K\|_{M(\Omega_o)} = K$.

It remains to show that for a given K the associated Lagrange multiplier denoted by $\beta(K)$ is positive, unique, and $\beta(K_1) \leq \beta(K_2)$ if $K_2 > K_1$. To prove the positivity, assume that $\beta(K) = 0$. Then we obtain

$$L(\bar{\omega}^K, \beta(K)) = \inf_{\omega \in M^+(\Omega_o)} L(\omega, \beta(K)) = \inf_{\omega \in M^+(\Omega_o)} \psi(\omega).$$

Given $\omega \in \mathrm{dom}_{M^+(\Omega_o)} \psi$, we have $\psi(2\omega) < \psi(\omega)$ and consequently the infimum in the equality above is not attained, yielding a contradiction. Assume that $\beta(K)$ is not unique, i.e. there exist $\beta_1(K), \beta_2(K) > 0$ such that each optimal solution $\bar{\omega}^K$ of (P^K) is also a minimizer of $L(\cdot, \beta_1(K))$ and $L(\cdot, \beta_2(K))$ over $M^+(\Omega_o)$. First we note again that $0 \in M^+(\Omega_o)$ is not an optimal solution to (P^K) due to the strict monotonicity of Ψ. Additionally it holds $\|\bar{\omega}^K\|_{M(\Omega_o)} = K$. Without loss of generality assume that $\beta_1(K) < \beta_2(K)$. From the necessary optimality conditions for $(P_{\beta_1(K)})$ and $(P_{\beta_2(K)})$, see (3.5), we then obtain

$$-\psi'(\bar{\omega}^K) \leq \beta_1(K) < \beta_2(K), \quad \operatorname{supp} \bar{\omega}_\beta \subset \left\{ x \in \Omega_o \mid -\psi'(\bar{\omega}_\beta)(x) = \beta_2(K) \right\},$$

implying $\bar{\omega}^K = 0$ which gives a contradiction. □

Many commonly used optimality criteria Ψ are positively homogeneous in the sense that there exists a convex, strictly decreasing, and positive function γ fulfilling

$$\Psi(rN) = \gamma(r)\,\Psi(N) \quad \forall r > 0,\ N \in \mathrm{PD}(n); \tag{3.7}$$

cf. also [27, p. 26]. For example, both the A and the D-criterion fulfill this homogeneity with γ_A and γ_D given by

$$\gamma_A(r) = r^{-1}, \quad \gamma_D(r) = r^{-n}.$$

The following lemma illustrates the findings of the previous result, provided that $\mathcal{I}_0 = 0$. It turns out that solutions to (P^K) can be readily obtained by scaling optimal solutions to (P_β).

Proposition 3.9. *Assume that $\mathcal{I}_0 = 0$ and Ψ is positive homogeneous in the sense of* (3.7). *Let $\bar{\omega}_\beta$ be a solution to (P_β) for some fixed $\beta > 0$. Then*

$$K\,\bar{\omega}_\beta / \|\bar{\omega}_\beta\|_{M(\Omega)} \quad \textit{solves} \quad (P^K). \tag{3.8}$$

Proof. First we note that under the stated assumptions every optimal solution $\bar{\omega}^K$ to (P^K) fulfills $\|\bar{\omega}^K\|_{M(\Omega_o)} = K$. Clearly, we have

$$\min(P^K) = \min_{\substack{\omega \in M^+(\Omega_o),\\ \|\omega\| = K}} \psi(\omega) = \min_{\substack{\omega' \in M^+(\Omega_o),\\ \|\omega'\| = 1}} \psi(K\omega') = \gamma(K)\min(P^1),$$

by using the positive homogeneity of Ψ. Thus, the solutions of (P^K) are given by $K\omega^1$, where ω^1 are solutions of (P^1). Now, using the fact that

$$\min(P_\beta) = \min_{K \geq 0} \left[\min_{\omega' \in M^+(\Omega_o),\ \|\omega'\| = 1} \psi(K\omega') + \beta K \right] = \min_{K \geq 0} \left[\gamma(K)\min(P^1) + \beta K \right]$$

the solutions $\bar{\omega}_\beta$ of (P_β) can be computed as $\bar{\omega}_\beta = K\omega^1$, where K minimizes the above expression and $\omega^1 \in \arg\min(P^1)$. Together, this directly implies (3.8). □

As we have shown in the case $\mathcal{I}_0 = 0$, i.e. in the absence of a priori knowledge, the optimal locations of the sensors x are independent of the cost parameter β (resp, K), which only affects the scaling of the coefficients λ. However for $\mathcal{I}_0 \neq 0$ this is generally not the case. Loosely speaking, if the a priori information is relatively good (i.e. $\mathcal{I}_0 \in \mathrm{PD}(n)$) and the cost per measurement is too high, the optimal design is given by the zero function, i.e. the experiment should not be carried out at all.

Proposition 3.10. *Let $\mathcal{I}_0 \in \mathrm{PD}(n)$. Then the zero function $\bar{\omega} = 0$ is an optimal solution to (P_β) if and only if $\beta > \beta_0 = -\min_{x \in \Omega_o} \psi'(0)$.*

Proof. We first note that $0 \in \operatorname{dom}\psi$ and $\beta_0 = -\min_{x \in \Omega_o} \psi'(0) < \infty$. Clearly, for $\beta \geq \beta_0$, the zero function fulfills the optimality conditions from Lemma 3.5. Thus, it is a solution to (P_β). Conversely, for $\beta < \beta_0$, the optimality conditions are violated. □

4. Algorithmic solution

In this section we will elaborate on the solution of (P_β). We consider two different approaches. First, we present an algorithm relying on finitely supported iterates and the sequential insertion of single Dirac Delta functions based on results for a linear-quadratic optimization problem in [16] and [15]. We derive all necessary results to prove convergence of the generated sequence of measures towards a minimizer of (P_β) together with a sublinear convergence rate of the objective function value. Additionally we propose to alternate

between point insertion and point deletion steps to benefit the sparsity of the iterates and to speed up the convergence of the algorithm in practice. These sparsification steps are based on the approximate solution of finite dimensional optimization problems in every iteration. As an example we give two explicit realizations for the point removal and discuss the additional computational effort in comparison to an algorithm solely based on point insertion steps. Moreover the resulting algorithms can be combined with Algorithm 1 in a straightforward manner, guaranteeing a sparse structure of the computed optimal design.

Secondly, we adapt an approach based on a Hilbert space regularization of the original sparse optimization problem. Here, the optimal design problem (P_β) is replaced by a sequence of regularized optimization problems, which are amenable to proximal point or semismooth Newton methods (which converge locally superlinearly). Algorithmic approaches for the solution of non-smooth optimization problems based on Hilbert space regularizations have recently increased in interest in the context of PDE-constrained optimization; see, e.g., [49, 21]. We briefly describe this approach for the sake of comparison at the end of this section.

4.1. **A generalized conditional gradient method.** For the direct solution of (P_β) on the admissible set $M^+(\Omega_o)$ we adapt the numerical procedure presented in [16], which relies on finitely supported iterates. A general description of the method is given in Algorithm 2. For convenience of the reader we give a detailed description of the individual steps and their derivation. The basic idea behind the procedure relies on a point insertion process (steps 2.–

Algorithm 2 Successive point insertion

1. Choose $\omega^1 \in \operatorname{dom}_{M^+(\Omega_o)} \psi$, $\#\operatorname{supp}\omega^1 \leq n(n+1)/2$. Set $M_0 = F(\omega^1)/\beta$.

while $\Phi(\omega^k) \geq \mathrm{TOL}$ **do**

2. Compute $\psi_k' = \psi'(\omega^k)$. Determine $\hat{x}^k \in \arg\min_{x\in\Omega_o} \psi_k'(x)$.
3. Set $v^k = \theta^k \delta_{\hat{x}^k}$ with $\theta^k = \begin{cases} 0, & \psi_k'(\hat{x}^k) \geq -\beta, \\ -(M_0/\beta)\psi_k'(\hat{x}^k), & \text{else} \end{cases}$
4. Select a step size $s^k \in (0,1]$ and set $\omega^{k+1/2} = (1-s^k)\omega^k + s^k v^k$.
5. Find ω^{k+1} with $\operatorname{supp}\omega^{k+1} \subseteq \operatorname{supp}\omega^{k+1/2}$ and $F(\omega^{k+1}) \leq F(\omega^{k+1/2})$.

end while

4. in Algorithm 2) related to a generalized conditional gradient method. More precisely, they consist of conditional gradient steps for a surrogate optimization problem with the same optimal solutions, in which the sublinear total variation norm is replaced by a coercive cost term for designs of very large norm. Additionally, we consider the minimization of the finite dimensional subproblem that arises from restriction of the design measure to the active support of the current iterate (in step 5.). This is motivated on the one hand by the desire to potentially remove non-optimal support points by setting the corresponding coefficient to zero, and on the other hand by the desire to obtain an accelerated convergence behavior in practice.

This section is structured as follows: First, we focus on the point insertion step and its descent properties. By a suitable choice of the step size s^k in each step of the procedure we are able to prove a sub-linear convergence rate for the objective functional value. Secondly, we consider two concrete examples for the point removal step 5. and discuss the applicability of Algorithm 1 in the context of the successive point insertion algorithm.

4.1.1. *Convergence analysis.* As already pointed out, Algorithm 2 relies on a coercive surrogate design problem which admits the same optimal solutions as (P_β). Given a constant $M_0 > 0$, we start by introducing the auxiliary function $\varphi_{M_0}\colon \mathbb{R}_+ \to \mathbb{R}$ as

$$\varphi_{M_0}(t) = \begin{cases} t, & t \leq M_0, \\ (1/(2M_0))\left[t^2 + M_0^2\right], & \text{else}, \end{cases}$$

and consider the modified problem

$$\min_{\omega \in M^+(\Omega_o)} F_{M_0}(\omega) = \psi(\omega) + \beta\varphi_{M_0}(\|\omega\|_{M(\Omega_o)}) \tag{$P_\beta^{M_0}$}$$

for the special choice of $M_0 = F(\omega^1)/\beta$, with arbitrary but fixed $\omega^1 \in \operatorname{dom}_{M^+(\Omega_o)} \psi$. Note that there holds $\|\omega\|_{M(\Omega_o)} \leq M_0$ and consequently $F(\omega) = F_{M_0}(\omega)$ for all $\omega \in M^+(\Omega_o)$ with $F(\omega) \leq F(\omega^1)$. We additionally point out that

$$\varphi_{M_0}(\|\bar{\omega}_\beta\|_{M(\Omega_o)}) = \|\bar{\omega}_\beta\|_{M(\Omega_o)} \tag{4.1}$$

for every optimal solution $\bar{\omega}_\beta$ of $(P_\beta^{M_0})$. Connected to this auxiliary problem we additionally define the primal-dual gap $\Phi\colon \operatorname{dom}\psi \to [0,\infty)$ by

$$\Phi(\omega) = \sup_{v \in M^+(\Omega_o)} \left[\langle \psi'(\omega), \omega - v\rangle + \beta\|\omega\|_{M(\Omega_o)} - \beta\varphi_{M_0}(\|v\|_{M(\Omega_o)})\right].$$

Note that the value of Φ is finite for every $v \in \operatorname{dom}\psi$, which follows with the coercivity of $\varphi_{M_0}(\cdot)$. In the next proposition we collect several results to establish the connection between the optimal design problems (P_β) and $(P_\beta^{M_0})$.

Proposition 4.1. *Let $\omega^1 \in \operatorname{dom}_{M^+(\Omega_o)} \psi$ be arbitrary but fixed and set $M_0 = F(\omega^1)/\beta$. Given $\bar{\omega}_\beta \in \operatorname{dom}_{M^+(\Omega_o)} \psi$ the following three statements are equivalent:*

- *1. The measure $\bar{\omega}_\beta$ is a minimizer of (P_β).*
- *2. The measure $\bar{\omega}_\beta$ is a minimizer of $(P_\beta^{M_0})$.*
- *3. The measure $\bar{\omega}_\beta$ fulfils $\Phi(\bar{\omega}_\beta) = 0$.*

Furthermore there holds

$$\Phi(\omega) \geq F(\omega) - F(\bar{\omega}_\beta) =: r_F(\omega), \tag{4.2}$$

for all $\omega \in \operatorname{dom}_{M^+(\Omega_o)} \psi, \|\omega\|_{M(\Omega_o)} \leq M_0$ and all minimizers $\bar{\omega}_\beta$ of $(P_\beta^{M_0})$.

Proof. The equivalence between the first two statements can be proven as in [16]. We only prove the third one. Similar to the proof of (3.4) (see Proposition 3.4) a given $\bar{\omega}_\beta \in \operatorname{dom}_{M^+(\Omega_o)} \psi$ is a minimizer of $(P_\beta^{M_0})$ if and only if it fulfills

$$-\langle \psi'(\bar{\omega}_\beta), \omega - \bar{\omega}_\beta\rangle + \beta\varphi_{M_0}(\|\bar{\omega}_\beta\|_{M(\Omega_o)}) \leq \beta\varphi_{M_0}(\|\omega\|_{M(\Omega_o)}) \quad \forall \omega \in M^+(\Omega_o).$$

By reordering and taking the minimum over all $\omega \in M^+(\Omega_o)$ this can be equivalently written as

$$\sup_{\omega \in M^+(\Omega_o)} \left[\langle \psi'(\bar{\omega}_\beta), \bar{\omega}_\beta - \omega\rangle + \beta\varphi_{M_0}(\|\bar{\omega}_\beta\|_{M(\Omega_o)}) - \beta\varphi_{M_0}(\|\omega\|_{M(\Omega_o)})\right] = 0.$$

Utilizing (4.1) we find $\Phi(\bar{\omega}_\beta) = 0$ if and only if $\bar{\omega}_\beta$ is a minimizer of F_{M_0}. It remains to prove (4.2). Given $\omega \in \operatorname{dom}_{M^+(\Omega_o)} \psi$ with $\|\omega\|_{M(\Omega_o)} \leq M_0$ and a minimizer $\bar{\omega}_\beta$ we obtain

$$F(\omega) - F(\bar{\omega}_\beta) \leq \beta\|\omega\|_{M(\Omega_o)} - \beta\|\bar{\omega}_\beta\|_{M(\Omega_o)} + \langle \psi'(\omega), \omega - \bar{\omega}_\beta\rangle, \tag{4.3}$$

by convexity of ψ. Noting that

$$-[\beta\|\bar{\omega}_\beta\|_{M(\Omega_o)} + \langle\psi'(\omega), \bar{\omega}_\beta\rangle] \leq -\inf_{v\in M^+(\Omega_o)}[\langle\psi'(\omega), v\rangle + \beta\varphi_{M_0}(\|v\|_{M(\Omega_o)})],$$

the right-hand side in (4.3) is estimated by $\Phi(\omega)$, which concludes the proof. □

With the result of the last proposition we may consider a minimization algorithm for $(P_\beta^{M_0})$ in order to compute optimal solutions to (P_β). Additionally, the result suggests the use of Φ as a convergence criterion, since it gives an upper bound for the residual error in the objective function value. As can be seen below, the evaluation of Φ can be easily computed as a by-product of steps 2.–3. in Algorithm 2.

The algorithm operates on finitely supported iterates $\omega^k = \sum_{i=1}^{m_k} \lambda_i^k \delta_{x_i^k}$ with distinct support points $x_i^k \in \Omega_o$ and positive coefficients λ_i^k, $i \in \{1, \dots, m_k\}, m_k \in \mathbb{N}$. A decrease of the objective function value in every iteration will be ensured, which implies

$$\beta\|\omega^{k+1}\|_{M(\Omega_o)} \leq F_{M_0}(\omega^{k+1}) \leq F_{M_0}(\omega^k) \leq F_{M_0}(\omega^1),$$

and consequently $F_{M_0}(\omega^k) = F(\omega^k)$ for all iterates ω^k. In steps 2.–4. the intermediate iterate $\omega^{k+1/2}$ is obtained as a convex combination between the previous iterate ω^k and a scaled Dirac delta function $\theta^k\delta_{\hat{x}^k}$ inserted at the global minimum of the gradient $\psi'(\omega^k)$. The initial coefficient θ^k is determined by the current maximal violation of the lower bound on the gradient of ψ; see (3.5). In the following lemma we relate this definition to the computation of a descent direction in the context of a generalized conditional gradient method (cf. [46, 16, 15]) for the auxiliary problem $(P_\beta^{M_0})$.

Lemma 4.2. *Let $\omega^k \in \operatorname{dom}_{M^+(\Omega_o)}\psi$ be given. Then the measure $v^k = \theta^k\delta_{\hat{x}^k}$ with $\hat{x}^k \in \Omega_o$ and $\theta^k \geq 0$ as defined in steps 2.–3. of Algorithm 2 is a minimizer of*

$$\min_{v\in M^+(\Omega_o)} \langle\psi'(\omega^k), v\rangle + \beta\varphi_{M_0}(\|v\|_{M(\Omega_o)}). \tag{P_β^{lin}}$$

Moreover, v^k realizes the supremum in the definition of the primal-dual gap: it holds $\Phi(v^k) = \langle\psi'(\omega^k), \omega^k - v^k\rangle + \beta\|\omega^k\|_{M(\Omega_o)} - \beta\varphi_{M_0}(\|v^k\|_{M(\Omega_o)})$.

Proof. We note that (P_β^{lin}) can be equivalently expressed as

$$\min_{r\in[0,\infty)} \min_{\substack{\tilde{v}\in M^+(\Omega_o),\\ \|\tilde{v}\|_{M(\Omega_o)}=1}} r\langle\psi'(\omega^k), \tilde{v}\rangle + \beta\varphi_{M_0}(r) = \min_{r\in[0,\infty)} r \min_{x\in\Omega_o} \psi'(\omega^k) + \beta\varphi_{M_0}(r).$$

The concrete expression of v^k follows now by a straightforward computation using the positive homogeneity of the total variation norm and the definition of $\varphi_{M_0}(\cdot)$. Clearly, $\Phi(v^k)$ agrees to $-\min(P_\beta^{\mathrm{lin}})$ up to a constant value. □

Remark 3. At this point, replacing (P_β) by the equivalent formulation $(P_\beta^{M_0})$ is crucial. In fact, the partially linearized problem corresponding to the original problem

$$\min_{v\in M^+(\Omega_o)} \langle\psi'(\omega), v\rangle + \beta\|v\|_{M(\Omega_o)},$$

is either unbounded or has an unbounded solution set in the case $\min_{x\in\Omega_o}\psi'(\omega) \leq -\beta$.

Note that, as a by-product of the last result, the convergence criterion $\Phi(\omega^k)$ can be evaluated cheaply once the current gradient $\psi'(\omega^k)$, and its minimum point are calculated.

We form the intermediate iterate as convex combination $\omega^{k+1/2} = (1 - s^k)\omega^k + s^k v^k$ between the old iterate and the new sensor, where $s^k \in (0, 1]$ is suitably chosen. This ensures $\omega^{k+1/2} \in M^+(\Omega_o)$. The step size s^k will be chosen by the following generalization

of the well-known Armijo-Goldstein condition; see, e.g., [15]. This choice of the step size ensures a sufficient decrease of the objective function value in every iteration of Algorithm 2 and the overall convergence of the presented method. More precisely, for fixed $\gamma \in (0,1)$, $\alpha \in (0, 1/2]$, the step size is set to $s^k = \gamma^{n_k}$, where n_k is the smallest non-negative integer with

$$\alpha s^k \Phi(\omega^k) \leq F_{M_0}(\omega^k) - F_{M_0}(\omega^k + s^k(v^k - \omega^k)). \tag{4.4}$$

Note that given an arbitrary non-optimal $\omega^k \in \operatorname{dom}_{M^+(\Omega_o)} \psi$ with $\|\omega^k\|_{M(\Omega_o)} \leq M_0$ this choice of the step size s^k is always possible since the function $W\colon [0,1] \to \mathbb{R} \cup \{-\infty\}$

$$W(s) = \frac{F_{M_0}(\omega^k) - F_{M_0}(\omega^k + s(v^k - \omega^k))}{s\Phi(\omega^k)}, \tag{4.5}$$

fulfills $\lim_{s\to 0} W(s) \geq 1$, similarly to [15, Remark 2]. To obtain quantifiable estimates for the descent in the objective function value we impose additional regularity assumptions on Ψ' until the end of this section.

Assumption 3. Assume that Ψ' is Lipschitz-continuous on compact sets: Given a compact set $\mathcal{N} \subset \operatorname{dom} \Psi$ there exists $L_{\mathcal{N}} > 0$ with

$$\sup_{N_1, N_2 \in \mathcal{N}} \frac{\|\Psi'(N_1) - \Psi'(N_2)\|}{\|N_1 - N_2\|} \leq L_{\mathcal{N}}, \tag{4.6}$$

where $\|A\| = \|A\|_{\mathrm{Sym}(n)} = \sqrt{\operatorname{Tr}(AA^\top)}$ is the Frobenius norm.

Note that this additional assumption is fulfilled if the design criterion Ψ is two-times continuously differentiable on its domain. This is the case for, e.g., the already mentioned A and D-criterion , see Section 3.2. We immediately arrive at the following proposition.

Proposition 4.3. *Let Assumption 3 hold and let $\omega_1 \in \operatorname{dom}_{M^+(\Omega_o)} \psi$ be given. Define the associated sub-level set E_{ω^1} as*

$$E_{\omega^1} = \left\{ \omega \in M^+(\Omega_o) \mid F(\omega) \leq F(\omega^1) \right\}.$$

Then there exists L_{ω^1} such that

$$\sup_{\omega_1, \omega_2 \in E_{\omega^1}} \frac{\|\psi'(\omega_1) - \psi'(\omega_2)\|_{C(\Omega_o)}}{\|\omega_1 - \omega_2\|_{M(\Omega_o)}} \leq L_{\omega^1}. \tag{4.7}$$

Proof. First we observe that E_{ω^1} is convex, bounded, and weak* closed. Consequently the set of associated information matrices

$$\mathcal{I}(E_{\omega^1}) = \{\, \mathcal{I}(\omega) + \mathcal{I}_0 \mid \omega \in E_{\omega^1} \,\}$$

is compact. For $\omega_1, \omega_2 \in E_{\omega^1}$ we obtain

$$\begin{aligned}
\|\psi'(\omega_1) - \psi'(\omega_2)\|_{C(\Omega_o)} &= \|\mathcal{I}^* \Psi'(\mathcal{I}(\omega_1) + \mathcal{I}_0) - \mathcal{I}^* \Psi'(\mathcal{I}(\omega_2) + \mathcal{I}_0)\| \\
&\leq \|\mathcal{I}^*\|_{\mathrm{Sym}(n)\to C(\Omega_o)} \|\Psi'(\mathcal{I}(\omega_1) + \mathcal{I}_0) - \Psi'(\mathcal{I}(\omega_2) + \mathcal{I}_0)\| \\
&\leq L_{\mathcal{I}(E_{\omega^1})} \|\mathcal{I}^*\|_{\mathrm{Sym}(n)\to C(\Omega_o)} \|\mathcal{I}(\omega_1) - \mathcal{I}(\omega_2)\| \\
&\leq L_{\mathcal{I}(E_{\omega^1})} \|\mathcal{I}^*\|_{\mathrm{Sym}(n)\to C(\Omega_o)} \|\mathcal{I}\|_{M^+(\Omega_o)\to \mathrm{Sym}(n)} \|\omega_1 - \omega_2\|_{M(\Omega_o)},
\end{aligned}$$

completing the proof. □

Using this additional local regularity we obtain the following estimate on the growth behavior of the function F at ω^k in the search direction.

Lemma 4.4. *Assume that Ψ' fulfills* (4.6). *Let $\omega^k \in \operatorname{dom}_{M^+(\Omega_o)} \psi$ with $\|\omega^k\|_{M(\Omega_o)} \leq M_0$ and v^k as in Lemma 4.2 be given. Moreover, define $\omega^{k+1/2} = (1-s^k)\omega^k + s^k v^k$ with s^k determined from* (4.4). *Then there holds*

$$F_{M_0}(\omega^{k+1/2}) - F_{M_0}(\omega^k) \leq -s^k \Phi(\omega^k) + \frac{L_{\omega^k}}{2} s^{k^2} \|v^k - \omega^k\|^2_{M(\Omega_o)},$$

where L_{ω^k} denotes the Lipschitz constant of ψ' on E_{ω^k}.

Proof. By choosing s^k from (4.4) there holds $F_{M_0}(\omega^{k+1/2}) \leq F_{M_0}(\omega^k)$ and consequently $\omega^{k+1/2} \in E_{\omega^k}$. Therefore we obtain

$$\begin{aligned} F_{M_0}(\omega^{k+1/2}) - F_{M_0}(\omega^k) &= -s^k \langle \psi'(\omega^k), \omega^k - v^k \rangle \\ &\quad + \beta \varphi_{M_0}(\|\omega^{k+1/2}\|_{M(\Omega_o)}) - \beta \varphi_{M_0}(\|\omega^k\|_{M(\Omega_o)}) + \int_0^{s^k} \langle \psi'(\omega_\sigma) - \psi'(\omega^k), v^k - \omega^k \rangle \, \mathrm{d}\sigma, \end{aligned}$$

with $\omega_\sigma = \omega^k + \sigma(v^k - \omega^k)$ for $\sigma \in [0,1]$. Using the convexity of $\varphi_{M_0}(\|\cdot\|_{M(\Omega_o)})$ we obtain

$$\begin{aligned} - s^k \langle \psi'(\omega^k), \omega^k - v^k \rangle + \beta \varphi_{M_0}(\|\omega^{k+1/2}\|_{M(\Omega_o)}) - \beta \varphi_{M_0}(\|\omega^k\|_{M(\Omega_o)}) \\ \leq -s^k \left(\langle \psi'(\omega^k), \omega^k - v^k \rangle + \varphi_{M_0}(\omega^k) - \varphi_{M_0}(v^k) \right), \end{aligned}$$

where the right-hand side simplifies to $-s^k \Phi(\omega^k)$. Due to the Lipschitz continuity of ψ' on E_{ω^k} we get

$$\begin{aligned} \int_0^{s^k} \langle \psi'(\omega_\sigma) - \psi'(\omega^k), v^k - \omega^k \rangle \, \mathrm{d}\sigma &\leq \|v^k - \omega^k\|_{M(\Omega_o)} \int_0^{s^k} \|\psi'(\omega_\sigma) - \psi'(\omega^k)\|_{C(\Omega_o)} \, \mathrm{d}\sigma \\ &\leq L_{\omega^k} \|v^k - \omega^k\|^2_{M(\Omega_o)} \int_0^{s^k} \sigma \mathrm{d}\sigma = \frac{L_{\omega^k}(s^k)^2}{2} \|v^k - \omega^k\|^2_{M(\Omega_o)}. \end{aligned}$$

Combining both estimates yields the result. □

In order to prove the main result we additionally need the following technical lemma.

Lemma 4.5. *Let $\omega^k \in \operatorname{dom}_{M^+(\Omega_o)} \psi$ with $\Phi(\omega^k) > 0$ be given. The function $W\colon (0,1] \to \mathbb{R} \cup \{-\infty\}$ from* (4.5) *is continuous on* $(0,1)$. *Furthermore, denoting by s^k the step size from* (4.4), *there exists $\hat{s}^k \in [s^k, s^k/\gamma]$ with $W(\hat{s}^k) = \alpha$ if $s^k < 1$.*

Proof. First, note that for $s \in [0,1)$ we have $\omega_s = (1-s)\omega^k + s v^k \in \operatorname{dom}_{M^+(\Omega_o)} \psi$ due to $\mathcal{I}(\omega_s) + \mathcal{I}_0 = (1-s)\,\mathcal{I}(\omega^k) + s\theta_k\, \partial S[\hat{q}](\hat{x}^k) \partial S[\hat{q}](\hat{x}^k)^\top + \mathcal{I}_0 \in \mathrm{PD}(n)$. Furthermore, using Assumption 2 it can be verified that

$$W(s) = (F_{M_0}(\omega_0) - F_{M_0}(\omega_s))/(s\,\Phi(\omega_0))$$

is continuous on $s \in (0,1)$. Additionally, with lower semi-continuity of Ψ, we verify that $W(s) \to -\infty$ for $s \to 1$ in case that $\mathcal{I}(v^k) \notin \operatorname{dom} \Psi$. We conclude the proof by applying the mean value theorem on $[s^k, s^k/\gamma] \subset (0,1]$, taking into account that $W(s^k) \geq \alpha > W(s^k/\gamma)$. □

Combining the previous results we are able to prove sub-linear convergence of the presented algorithm.

Theorem 4.6. *Let the sequence ω^k be generated by Algorithm 2 using the Quasi-Armijo-Goldstein condition* (4.4)*. Then there exists at least one weak* accumulation point $\bar{\omega}_\beta$ of ω^k and every such point is an optimal solution to (P_β). Additionally there holds*

$$r_F(\omega^k) \leq \frac{r_F(\omega^1)}{1+q(k-1)} \tag{4.8}$$

with

$$q = \alpha \min\left\{ \frac{c_1}{L_{\omega^1}(M_0+c_2)^2},\ 1 \right\}, \tag{4.9}$$

where L_{ω^1} is the Lipschitz-constant of ψ' on E_{ω^1}, $M_0 = F(\omega^1)/\beta$, $c_1 = 2\gamma(1-\alpha)r_F(\omega_1)$ and a constant $c_2 > 0$ with $\|v^k\|_{M(\Omega_o)} \leq c_2$ for all k.

Proof. Assume without restriction that $\Phi(\omega^k) > 0$, i.e. the algorithm does not terminate after finitely many steps. By construction and the choice of s^k there holds $\omega^k \in E_{\omega^1}$ and consequently $\|\omega^k\|_{M(\Omega_o)} \leq M_0$, $F_{M_0}(\omega^k) = F(\omega^k)$ for all k. The same can be proven for $\omega^{k+1/2}$. Note that ω^k is bounded and ψ' is weak*-to-strong continuous. Therefore, there exists $c_2 > 0$ with $\|v^k\|_{M(\Omega_o)} \leq c_2$ for all k s.

Due to the boundedness of ω^k there exists a subsequence denoted by the same symbol with weak* limit $\bar{\omega}_\beta$. By the definition of the step size s^k as well as (4.2) there holds

$$\alpha s^k r_F(\omega^k) \leq \alpha s^k \Phi(\omega^k) \leq r_F(\omega^k) - r_F(\omega^{k+1/2}),$$

which yields

$$r_F(\omega^{k+1/2}) \leq (1-\alpha s^k) r_F(\omega^k). \tag{4.10}$$

Since $\Phi(\omega^k) > 0$ we obtain $s^k \neq 0$ for all k. Two cases have to be distinguished. If s^k is equal to one we immediately arrive at

$$r_F(\omega^{k+1/2}) \leq (1-\alpha) r_F(\omega^k) \leq r_F(\omega^k) - \alpha \frac{r_F(\omega^k)^2}{r_F(\omega^1)}.$$

In the second case, if $s^k < 1$, there exists $\hat{s}^k \in [s^k, s^k/\gamma]$ with

$$\alpha = \frac{F(\omega^k) - F(\omega^k + \hat{s}^k(v^k - \omega^k))}{\hat{s}^k \Phi(\omega^k)},$$

using Lemma 4.5. Consequently $\omega^k + s(v^k - \omega^k) \in E_{\omega^1}$ for all $0 \leq s \leq \hat{s}^k$ due to the convexity of F. Because of the Lipschitz-continuity of ψ' on E_{ω_1}, Lemma 4.4 can be applied and, defining $\delta\omega^k = v^k - \omega^k$, there holds

$$\alpha = \frac{F(\omega^k) - F(\omega^k + \hat{s}^k \delta\omega^k)}{\hat{s}^k \Phi(\omega^k)} \geq 1 - \frac{L_{\omega^1}\hat{s}^k}{2} \frac{\|\delta\omega^k\|^2_{M(\Omega_o)}}{\Phi(\omega^k)} \geq 1 - \frac{L_{\omega^1} s^k}{2\gamma} \frac{\|\delta\omega^k\|^2_{M(\Omega_o)}}{\Phi(\omega^k)}.$$

The last estimate is true because of $\hat{s}^k \leq s^k/\gamma$. Reordering and using(4.2) yields

$$1 \geq s^k \geq 2\gamma(1-\alpha)\frac{\Phi(\omega^k)}{L_{\omega^1}\|v^k - \omega^k\|^2_{M(\Omega_o)}} \geq 2\gamma(1-\alpha)\frac{r(\omega^k)}{L_{\omega^1}\|v^k - \omega^k\|^2_{M(\Omega_o)}}.$$

Combining the estimates in both cases and using $r_F(\omega^{k+1}) \geq r_F(\omega^{k+1/2})$, the inequality

$$0 \leq \frac{r_F(\omega^{k+1})}{r_F(\omega^1)} \leq \frac{r_F(\omega^{k+1/2})}{r_F(\omega^1)} \leq \frac{r_F(\omega^k)}{r_F(\omega^1)} - q_k \left(\frac{r_F(\omega^k)}{r_F(\omega^1)}\right)^2 \quad \forall k \in \mathbb{N} \tag{4.11}$$

holds, where the constant q_k is given by

$$q_k = r_F(\omega^1)\alpha \min\left\{\frac{2\gamma(1-\alpha)}{L_{\omega^1}\|v^k-\omega^k\|^2_{M(\Omega_o)}}, \frac{1}{r_F(\omega^k)}\right\} \geq \alpha \min\left\{\frac{2\gamma(1-\alpha)r_F(\omega^1)}{L_{\omega^1}(M_0+c_2)^2}, 1\right\} =: q,$$

if $s^k < 1$ and $q_k = \alpha$ otherwise. The claimed convergence rate (4.8) now follows directly from the recursion formula (4.11); see [23, Lemma 3.1]. Consequently each subsequence of ω^k is a minimizing sequence and each weak* accumulation point $\bar{\omega}_\beta$ is a minimizer of (P_β) due to the weak* lower semi-continuity of F. □

4.2. **Acceleration and sparsification strategies.** As we have seen in the previous section, an iterative application of steps 2.–4. in Algorithm 2 is sufficient to obtain weak* convergence of the iterates ω^k, as well as a sublinear convergence rate for the objective function. However, it is obvious that the support size of the iterates ω^k grows monotonically in every iteration unless the current gradient is bounded from below by $-\beta$ or, more unlikely, the step size s^k is chosen as 1. Therefore, while the implementation of steps 2.–4. is fairly easy, an algorithm only consisting of point insertion steps will likely yield iterates with undesirable sparsity properties, e.g., a clusterization of the intermediate support points around the support points of a minimizer to (P_β). In the following we mitigate those effects by augmenting the point insertion steps by point removal steps, where we incorporate ideas from [16, 13]. We define the parameterization:

$$\boldsymbol{\omega}(\lambda) := \sum_{x_i \in \operatorname{supp}\omega^{k+1/2}} \lambda_i \delta_{x_i} \quad \forall \lambda \in \mathbb{R}^{m_k},\ m_k = \#\operatorname{supp}\omega^{k+1/2}. \tag{4.12}$$

Now, we set $\omega^{k+1} = \boldsymbol{\omega}(\lambda^{k+1})$, where the improved vector $\lambda^{k+1} \in \mathbb{R}^{m_k}$ is chosen as an approximate solution to the (finite dimensional) coefficient optimization problem

$$\min_{\lambda\in\mathbb{R}^{m_k},\ \lambda\geq 0} F(\boldsymbol{\omega}(\lambda)) = \psi(\boldsymbol{\omega}(\lambda)) + \beta\|\lambda\|_1, \tag{4.13}$$

that fulfills $F(\omega^{k+1}) \leq F(\omega^{k+1/2})$. In this manuscript, we focus on two special instances of this removal step, which are detailed below.

In the first strategy, the new coefficient vector $\lambda^{k+1} = \lambda^{k+1}(\sigma_k)$ is obtained by

$$\lambda^{k+1}(\sigma_k)_i = \max\left\{\lambda_i^{k+1/2} - \sigma_k\left[\psi'(\omega^{k+1/2})(x_i) + \beta\right],\ 0\right\} \quad \forall i \in \{1,\dots,m_k\}, \tag{4.14}$$

where $\sigma_k > 0$ is a suitably chosen step size that avoids ascend in the objective function value. This corresponds to performing one step of a projected gradient method on (4.13) using the previous coefficient vector $\lambda^{k+1/2}$ as a starting point. Thus, step 5. in Algorithm 2 subtracts or adds mass at support point x_i for $-\psi'(\omega^{k+1/2})(x_i) < \beta$ or $-\psi'(\omega^{k+1/2})(x_i) > \beta$, respectively. Furthermore, the new coefficient λ_i^{k+1} of the Dirac delta function δ_{x_i} is set to zero if

$$\lambda_i^{k+1/2} - \sigma_k(\psi'(\omega^{k+1/2})(x_i) + \beta) \leq 0,$$

removing the point measure from the iterate.

Secondly, we suppose that the finite-dimensional sub-problems (4.13) can be solved exactly and choose

$$\lambda^{k+1} \in \operatorname*{arg\,min}_{\lambda\in\mathbb{R}^{m_k},\ \lambda\geq 0} F(\boldsymbol{\omega}(\lambda)). \tag{4.15}$$

In this case, the conditions

$$\operatorname{supp}\omega^{k+1} \subset \operatorname{supp}\omega^{k+1/2}, \quad F(\omega^{k+1}) \leq F(\omega^{k+1/2})$$

are trivially fulfilled. If all finite dimensional sub-problems are solved exactly, the method can be interpreted as a method operating on a set of active points $\mathcal{A}_k = \operatorname{supp}\omega^k$; cf. [43]: In each iteration, the minimizer $\hat{x}^k$ of the current gradient ψ'_k is added to the support set to obtain $\mathcal{A}_{k+1/2} = \mathcal{A}_k \cup \{\,\hat{x}^k\,\}$. Then, the problem (4.15) is solved on the new support set (i.e. with $\operatorname{supp}\omega^{k+1/2}$ replaced by $\mathcal{A}_{k+1/2}$ in the definition of (4.12)) to obtain the next iterate ω^{k+1}. Note that the next active set is given by $\mathcal{A}_{k+1} = \operatorname{supp}\omega^{k+1}$, which automatically removes support points corresponding to zero coefficients in each iteration.

Finally, to be able to guarantee the a priori bound $\#\operatorname{supp}\omega^k \leq n(n+1)/2$ for the algorithmic solutions, we can apply Algorithm 1 to the intermediate iterate $\omega^{k+1/2}$ in step 5. of Algorithm 2. This ensures the convergence of the presented procedure towards a sparse minimizer of (P_β).

Proposition 4.7. *Assume that* $\#\operatorname{supp}\omega^1 \leq n(n+1)/2$ *and let* ω^{k+1} *be obtained by applying Algorithm 1 to* $\omega^{k+1/2}$ *in each iteration of Algorithm 2. Then the results of Theorem 4.6 hold. Furthermore we obtain* $\#\operatorname{supp}\omega^k \leq n(n+1)/2$ *for all* $k \in \mathbb{N}$ *and consequently* $\#\operatorname{supp}\bar{\omega}_\beta \leq n(n+1)/2$ *for every weak* accumulation point* $\bar{\omega}_\beta$ *of* ω^k.

Proof. The statement for the support of ω^k readily follows from an inductive application of Proposition 3.7 by noting that

$$\left\{\, \mathcal{I}(\delta_x) \mid x \in \operatorname{supp}\omega^k \,\right\} \subset \operatorname{Sym}(n),$$

and $\dim \operatorname{Sym}(n) = n(n+1)/2$. The sparsity statement for every accumulation point $\bar{\omega}$ follows directly from the uniform bound on the number of support points in each of the iterates ω^k; see [43, Proposition C.1]. □

We emphasize that the sparsifying procedure from Algorithm 1 can be readily combined with the previously presented point removal steps in a straightforward fashion. In practical computations we optimize the coefficients of the Dirac delta functions in the current support either by (4.14) or (4.15) obtaining an intermediate iterate $\omega^{k+3/4}$. Subsequently we apply Algorithm 1. Since in both cases, the number of support points cannot increase, the statements of the last proposition remain true.

Remark 4. Note that Algorithm 2 can be easily generalized to allow for the insertion of more than one point in every iteration, which yields an additional practical speed up of the method; see Section 6.2.3. In detail, the results of Theorem 4.6 and Proposition 4.7 hold true if the search direction $v^k \in M^+(\Omega_o)$ from Lemma 4.2 is more generally chosen as

$$v^k = \sum_{i=1}^m \lambda_i \delta_{x_i}, \quad \{x_i\}_{i=1}^m \subset \operatorname*{arg\,min}_{x\in\Omega_o} \psi'(\omega^k), \quad \|v^k\|_{M(\Omega_o)} = -M_0 \min_{x\in\Omega_o} \psi'(\omega^k)/\beta$$

if $\min_{x\in\Omega_o} \psi'(\omega^k) \leq -\beta$. Moreover, in the case that all finite-dimensional sub-problems are solved exactly, all results remain valid if we compute ω^{k+1} as the solution of the coefficient minimization problem (4.15) with $\operatorname{supp}\omega^{k+1/2}$ replaced by some finite point set $\mathcal{A}_{k+1/2}$ which contains $\operatorname{supp}\omega^k \cup \{\,\hat{x}_k\,\}$.

4.3. **Computational cost of the sparsification steps.** It remains to comment on the computational cost associated with the various point removal steps presented in this section. First, we address the costs for the point removal steps based on the approximate solution of the finite dimensional subproblems. Computing the new coefficient vector λ^k from (4.14) requires the computation of the pointwise evaluation of $\psi'(\omega^{k+1/2})$ at the current support points once. In our numerical experiments a suitable step size σ_k is found by a simple

backtracking line search to avoid ascend. Consequently, for each trial step size, the max-operator in (4.14) as well as the objective function is evaluated once. This can be done efficiently with cost scaling linearly with the current support size m_k.

Secondly, if λ^k is determined from (4.15), we have to solve a finite-dimensional convex optimization problem in every iteration. Since the most common choices for the optimal design criterion Ψ are twice continuously differentiable, we choose to implement a semi-smooth Newton method. To benefit from the fast local convergence behavior for this class of methods we warm-start the algorithm using the coefficient vector $\lambda^{k+1/2}$ of the intermediate iterate $\omega^{k+1/2}$. This choice of the starting point often gives a good initial guess for λ^{k+1}. However, we emphasize that essentially any algorithm for smooth convex problems with positivity constraints on the optimization variables can be employed instead. In particular, interior point methods provide complexity bounds for the solution up to machine precision in terms of the support size m_k; see, e.g., [14, Section 11.5]. In light of this fact, the computational cost for the point removal steps can be regarded as a constant, assuming that m_k is uniformly bounded through the iterations, e.g., by employing Algorithm 1. However, interior point methods cannot be warm-started in general, which is why we prefer semi-smooth Newton methods in practice.

Finally, we consider the application of Algorithm 1, given a sparse input measure ω with $\operatorname{supp}\omega = \{x_i\}_{i=1}^m$. Step 1. amounts to the computation of the symmetric rank one matrices $\{\mathcal{I}(\delta_{x_i})\}_{i=1}^m \subset \mathrm{NND}(n)$, which we identify with vectors $\{\boldsymbol{I}(\delta_{x_i})\}_{i=1}^m \subset \mathbb{R}^{n(n+1)/2}$. Additionally, in each execution of the loop step 2. has to be executed, which requires to compute a vector $\bar{\lambda}$ in the kernel of the matrix $\boldsymbol{I}(\omega) \in \mathbb{R}^{n(n+1)/2\times m}$, defined by

$$[\boldsymbol{I}(\omega)]_{j,i} = \boldsymbol{I}(\delta_{x_i})_j, \quad i = 1,\dots,m,\ j = 1,\dots,n(n+1)/2.$$

This can be done efficiently employing either a SVD-decomposition or a rank-revealing QR-decomposition. Furthermore, assuming that Algorithm 1 is applied to $\omega^{k+1/2}$ for every k, this loop will run at most in each iteration. This can be seen in the following way: Let the k-th iterate ω^k in Algorithm 2 be given such that $\operatorname{rank}\boldsymbol{I}(\omega^k) = \#\operatorname{supp}\omega^k$. Note that this implies $\#\operatorname{supp}\omega^k \leq n(n+1)/2$. Consequently we have either $\operatorname{rank}\boldsymbol{I}(\omega^{k+1/2}) = \#\operatorname{supp}\omega^{k+1/2}$ or $\operatorname{rank}\boldsymbol{I}(\omega^{k+1/2}) = \#\operatorname{supp}\omega^{k+1/2} - 1$. In the first case no sparsification by the post-processing can be achieved. In the second case $\omega^{k+1/2} = \sum_{j=1}^m \lambda_j \delta_{x_j}$ is at least sparsified once. After the first execution of the sparsification loop, we obtain the measure $\omega_{\mathrm{new}} = \sum_{\{\, i \mid \lambda_{\mathrm{new},i}>0 \,\}} \lambda_{\mathrm{new},i}\delta_{x_i}$ with $\operatorname{rank}\boldsymbol{I}(\omega_{\mathrm{new}}) = \#\operatorname{supp}\omega_{\mathrm{new}}$, i.e. Algorithm 1 terminates.

4.4. **Algorithmic solution by path-following.** As an alternative to Algorithm 2, we briefly describe a path-following approach. To compute a minimizer of (P_β) we solve a sequence of regularized problems given by:

$$\min_{\omega\in L^2(\Omega_o))} \psi(\omega) + \beta\|\omega\|_{L^1(\Omega_o)} + \frac{\varepsilon}{2}\|\omega\|^2_{L^2(\Omega_o)}. \tag{P_β^ε}$$

In the limiting case for $\varepsilon \to 0$, the regularized optimal solutions approximate solutions of (P_β). We state first order optimality conditions for solutions of the regularized problem and investigate the case $\varepsilon \to 0$. For the sake of brevity, we omit most proofs.

Proposition 4.8. *Let the assumptions of Proposition 3.2 be fulfilled. Then the following statements hold:*

- *For every $\varepsilon > 0$ there exists a unique solution $\bar{\omega}_\beta^\varepsilon \in L^2(\Omega_o)$ to (P_β^ε).*

- *A non-negative function $\bar{\omega}_\beta^\varepsilon \in L^2(\Omega_o)$ is optimal if and only if*

$$\bar{\omega}_\beta^\varepsilon = \max\left\{-\frac{1}{\varepsilon}(\psi'(\bar{\omega}_\beta^\varepsilon)+\beta), 0\right\}. \tag{4.16}$$

  Consequently there holds $\bar{\omega}_\beta^\varepsilon \in C(\Omega_o)$ and

$$\bar{\omega}_\beta^\varepsilon(x) > 0 \text{ if and only if } -\psi'(\bar{\omega}_\beta^\varepsilon)(x) > \beta.$$

- *Given any sequence $\{\varepsilon_k\}_{k\in\mathbb{N}}$ with $\varepsilon_k > 0$, $\varepsilon_k \to 0$, the associated sequence $\bar{\omega}_\beta^{\varepsilon_k}$ admits at least one weak* accumulation point and every such point is an optimal solution to (P_β).*

Proof. By assumption there exists $\omega \in M^+(\Omega_o)$ with $\psi(\omega) < \infty$, i.e. $\mathcal{I}(\omega) + \mathcal{I}_0 \in \mathrm{PD}(n)$. Following [42, Appendix A.1], there exists a sequence $\{\omega_k\}_{k\in\mathbb{N}} \subset L^2(\Omega_o)$, $\omega_k \geq 0$ with $\omega_k \to^* \omega$. Consequently there also holds

$$\mathcal{I}(\omega_k) + \mathcal{I}_0 \to \mathcal{I}(\omega) + \mathcal{I}_0 \in \mathrm{PD}(n),$$

due to the weak*-to-strong continuity of $\mathcal{I}$. Thus we observe $\mathcal{I}(\omega) + \mathcal{I}_0 \in \mathrm{PD}(n)$ and $\psi(\omega_k) < \infty$ for all k large enough. The existence of at least one optimal solution $\bar{\omega}_\beta^\varepsilon$ now follows by similar arguments as in Proposition 3.2. Its uniqueness follows due to the strict convexity of F_ε. The necessary and sufficient optimality condition can be derived as in [49] and [18]. For the last result we observe that given an arbitrary positive null sequence $\{\varepsilon_k\}_{k\in\mathbb{N}}$ there holds

$$\beta\|\bar{\omega}_\beta^\varepsilon\|_{L^1(\Omega_o)} \leq F_{\varepsilon_k}(\bar{\omega}_\beta^{\varepsilon_k}) \leq F(\omega) + \frac{1}{2}\|\omega\|_{L^2(\Omega_o)}$$

for an arbitrary but fixed $\omega \in L^2(\Omega_o)$, $\omega \geq 0$ and all k large enough. Following the lines of the proof in [42, Section 2.5] existence of at least one weak* accumulation point of $\bar{\omega}_\beta^{\varepsilon_k}$ as well as its optimality for (P_β) can now easily be deduced. □

Note that for fixed $\varepsilon > 0$ the unique minimizer $\bar{\omega}_\beta^\varepsilon$ is a solution of

$$\omega - \max\left\{-\frac{1}{\varepsilon}(\psi'(\omega)(x)+\beta), 0\right\} = 0. \tag{4.17}$$

Under additional regularity assumptions on the optimal design criterion Ψ, the solution of this non-smooth operator equation can be computed by a semi-smooth Newton method in function space; see, e.g., [54]. To compute a solution for the original problem (P_β) we employ a continuation strategy for the regularization parameter ε. For an initial small value ε we compute the unique minimizer $\bar{\omega}_\beta^\varepsilon$ to (P_β^ε) by solving (4.17). Then, in an outer loop, we decrease ε, and use the previous optimal solution as an initial guess for the next iteration. The procedure is summarized in Algorithm 3. For further references on path-following we refer to, e.g., [32, 33, 34].

Algorithm 3 Path-following

1. Choose $\varepsilon_1 > 0$ and initial guess $\omega_\varepsilon^1 \in \mathrm{dom}_{M^+(\Omega_o)}\,\psi \cap L^2(\Omega_o)$.

while residual (4.17) large **do**

2. Compute $\bar{\omega}_\beta^{\varepsilon_l}$ from (4.17) using $\bar{\omega}_\beta^{\varepsilon_{l-1}}$ as initial guess.
3. Get $\varepsilon_{l+1} < \varepsilon_l$, $l = l + 1$.

end while

5. Discretization

In the following, the sets Ω as well as Ω_o are assumed to be polytopal (i.e. polygonal in two dimensions and polyhedral in three dimensions). We discuss the approximation of (P_β) by linear finite elements. For this purpose we consider a family of triangulations $\{\,\mathcal{T}_h\,\}_{h>0}$ of Ω with

$$\Omega = \bigcup_{T\in\mathcal{T}_h} \bar{T}, \quad \Omega_o = \bigcup_{T\in\mathcal{T}_h^o} \bar{T}, \tag{5.1}$$

where $\mathcal{T}_h^o \subset \mathcal{T}_h$ denotes the union of all cells making up the observational domain. We assume that the triangulation fulfills the usual regularity conditions (cf., e.g., [19]). By $\mathcal{N}_h$ we denote the set of nodes of the triangulation. For each $h > 0$ we now define the space of continuous piecewise linear finite elements V_h on $\mathcal{T}_h$ and its dual space $V_h^* \simeq M_h$ as

$$V_h = \{\, y_h \in C(\bar\Omega) \mid y_{h|T} \in P_1 \ \forall T \in \mathcal{T}_h \,\}, \quad M_h = \{\, \omega_h \in M(\bar\Omega) \mid \operatorname{supp}\omega_h \subset \mathcal{N}_h \,\}.$$

In the following assume that $Y_h = V_h \cap Y$ is not empty. For each $x_i \in \mathcal{N}_h$ we denote by $e_i^h \in V_h$ the associated nodal basis function. Finally, we introduce the nodal interpolation operators $i_h\colon C(\bar\Omega) \to V_h$ and $\Lambda_h\colon M(\bar\Omega) \to M_h$ as

$$i_h(y) = \sum_{x_i\in\mathcal{N}_h} y(x_i)e_i^h, \quad \Lambda_h(\omega) = \sum_{x_i\in\mathcal{N}_h} \langle e_i^h, \omega\rangle \delta_{x_i}$$

see, e.g., [17]. Note that $\Lambda_h\omega \in M^+(\Omega_o) \cap M_h$ for all $\omega \in M^+(\Omega_o)$ due to (5.1).

We define the discrete state space $\hat{Y}_h = \hat{y}_h + Y_h$ where $\hat{y}_h$ denotes an approximation of the Dirichlet boundary data $\hat{y}$. For a given $q \in Q_{ad}$ the discrete state equation $y^h = S^h[q]$ is defined as

$$y^h \in \hat{Y}_h \ \text{ such that } \ a(q, y^h)(\varphi_h) = 0 \quad \forall \varphi_h \in Y_h. \tag{5.2}$$

Analogously, for all $k \in \{\,1,\dots,n\,\}$, the discrete sensitivity $\delta y^h = \partial_k S^h[\hat{q}] \in Y_h \cap C(\Omega_o)$ at the given a priori guess $\hat{q}$ is given as the solution to

$$a'_y(\hat{q}, y^h)(\delta y^h, \varphi_h) = -a'_{q_k}(\hat{q}, \hat{y}^h)(\varphi_h) \quad \forall \varphi_h \in Y_h, \tag{5.3}$$

where $\hat{y}^h = S^h[\hat{q}]$. For the remainder of this section we make the following assumption.

Assumption 4. There exists $h_0 > 0$ such that for all $h \le h_0$ and $\hat{q} \in Q_{ad}$ the discrete state and sensitivity equations, (5.2) and (5.3), admit unique solutions. Moreover the discrete sensitivities fulfill

$$\lim_{h\to 0} \max_k \|\partial_k S[\hat{q}] - \partial_k S^h[\hat{q}]\|_{C(\Omega_o)} = 0.$$

Note that these assumptions can be verified for a variety of settings, in particular the ones considered in Section 6.

5.1. Discretization of (P_β).

We define the discrete approximation to (P_β) by

$$\min_{\omega_h\in M^+(\Omega_o)} F_h(\omega) = [\psi_h(\omega_h) + \beta\|\omega_h\|_{M(\Omega_o)}], \tag{$P_{\beta,h}$}$$

where $\psi_h(\omega_h) = \Psi(\mathcal{I}_h(\omega_h) + \mathcal{I}_0)$ and the operator $\mathcal{I}_h$ results from the discretization of the Fisher operator $\mathcal{I}$ as

$$\mathcal{I}_h\colon M(\Omega_o) \to \operatorname{Sym}(n), \quad \mathcal{I}_h(\omega_h)_{i,j} = \langle \partial_i S^h[\hat{q}]\partial_j S^h[\hat{q}], \omega_h\rangle. \tag{5.4}$$

Initially, we do not discretize the optimal design space $M^+(\Omega_o)$, which corresponds to a variational discretization approach; cf. [35, 18]. However, we will show below that this is essentially equivalent to an additional discretization of the measure space by M_h.

Turning to the study of $(P_{\beta,h})$, we observe that existence of at least one discrete optimal solution $\bar{\omega}_{\beta,h} \in M^+(\Omega_o)$ can be concluded in the same way as for the continuous problem (cf. Proposition 3.2), provided that the discrete sensitivities fulfill

$$\mathbb{R}^n = \operatorname{span}\left(\operatorname{Ran}\mathcal{I}_0 \cup \{\, \partial S^h[\hat{q}](x) \mid x \in \Omega_o \,\}\right).$$

Due to Assumption 4, this property of the discrete problem follows from the analogous property of the continuous problem for h small enough. In the next theorem we show that, in addition, there exists at least one discrete optimal solution located in the nodes of the triangulation.

Theorem 5.1. *Assume that $\partial S[\hat{q}]$ fulfills the assumptions from Proposition 3.3 and let Assumption 4 hold. Then there exists $h_0 > 0$ such that for every $h \le h_0$ the problem $(P_{\beta,h})$ admits at least one optimal solution $\bar{\omega}_{\beta,h} \in M^+(\Omega_o)$ fulfilling*

$$\psi_h'(\bar{\omega}_{\beta,h}) \ge -\beta, \quad \operatorname{supp}\bar{\omega}_{\beta,h} \subset \{x \in \Omega_o | -\psi_h'(\bar{\omega}_{\beta,h})(x) = \beta\},$$

and $\#\operatorname{supp}\bar{\omega}_{\beta,h} \le n(n+1)/2$. Moreover, for every optimal solution $\bar{\omega}_{\beta,h}$ of $(P_{\beta,h})$ the interpolated measure $\Lambda_h(\bar{\omega}_{\beta,h}) \in M_h$ is also optimal.

Proof. We have to show that the domain of ψ_h on $M^+(\Omega_o)$ is not empty for all h small enough, existence of at least one discrete optimal solution as well as the necessary and sufficient optimality conditions follow as for the continuous problem. By assumption there exists $\omega \in M^+(\Omega_o)$ with $\mathcal{I}(\omega) + \mathcal{I}_0 \in \mathrm{PD}(n)$. Due to the uniform convergence of the sensitivities $\partial S_h[q]$, we have $\mathcal{I}_h(\omega) \to \mathcal{I}(\omega)$ for $h \to 0$. Therefore, for h small enough there holds $\mathcal{I}_h(\omega) + \mathcal{I}_0 \in \mathrm{PD}(n)$, since the set of invertible matrices is open.

It remains to prove the existence of a solution supported in $\mathcal{N}_h$. Given an arbitrary but fixed $\omega \in M^+(\Omega_o)$ we have

$$\mathcal{I}_h(\Lambda_h\omega)_{ik} = \left\langle \partial_i S^h[\hat{q}]\partial_k S^h[\hat{q}], \Lambda_h\omega \right\rangle = \left\langle i_h\left(\partial_i S^h[\hat{q}]\partial_k S^h[\hat{q}]\right), \omega \right\rangle$$

for all $i, k \in \{1, \dots, n\}$, by using properties of Λ_h; see [17, Theorem 3.5]. Now, let $z \in \mathbb{R}^n$ be arbitrary. Then there holds

$$\begin{aligned} z^T \mathcal{I}_h(\omega) z = \left\langle z^\top \partial S^h[\hat{q}]\partial S^h[\hat{q}]^\top z, \omega \right\rangle &= \left\langle \left(\partial S^h[\hat{q}]^\top z\right)^2, \omega \right\rangle \\ &= \left\langle \left(\sum_{x_j \in \mathcal{N}_h} e_j^h \, \partial S^h[\hat{q}](x_j)^\top z \right)^2, \omega \right\rangle, \end{aligned}$$

using $\sum_{x_i \in \mathcal{N}_h} e_i^h(x) = 1$ for all $x \in \Omega_o$. Now, we estimate

$$\left\langle \left(\sum_{x_j \in \mathcal{N}_h} e_j^h z^\top \partial S^h[\hat{q}](x_j) \right)^2, \omega \right\rangle \le \left\langle \sum_{x_j \in \mathcal{N}_h} e_j^h \left(z^\top \partial S^h[\hat{q}](x_j) \right)^2, \omega \right\rangle,$$

with Jensen's inequality, using the convexity of the square function. Expanding and rearranging yields

$$\begin{aligned} \left\langle \sum_{x_j \in \mathcal{N}_h} e_j^h \left(z^\top \partial S^h[\hat{q}](x_j) \right)^2, \omega \right\rangle &= \left\langle \sum_{x_j \in \mathcal{N}_h} e_j^h \, z^\top \partial S^h[\hat{q}](x_j)\partial S^h[\hat{q}](x_j)^\top z, \omega \right\rangle \\ &= \left\langle i_h\left(z^\top \partial S^h[\hat{q}]\partial S^h[\hat{q}]^\top z\right), \omega \right\rangle = \left\langle z^\top \partial S^h[\hat{q}]\partial S^h[\hat{q}]^\top z, \Lambda_h\omega \right\rangle = z^T \mathcal{I}_h(\Lambda_h\omega) z. \end{aligned}$$

Since $z \in \mathbb{R}^n$ was arbitrary, this implies $\mathcal{I}_h(\omega) \leq_L \mathcal{I}_h(\Lambda_h\omega)$ and therefore also

$$\Psi(\mathcal{I}_h(\omega) + \mathcal{I}_0) \geq \Psi(\mathcal{I}_h(\Lambda_h\omega) + \mathcal{I}_0),$$

due to the monotonicity of Ψ with respect to the Löwner ordering. Let $\bar{\omega}_{\beta,h}$ be an optimal solution of $(P_{\beta,h})$. From this and $\|\Lambda_h\bar{\omega}_{\beta,h}\|_{M(\Omega_o)} \leq \|\bar{\omega}_{\beta,h}\|_{M(\Omega_o)}$ we deduce that $\Lambda_h\bar{\omega}_{\beta,h}$ is an optimal solution to $(P_{\beta,h})$. □

Note that this result, together with Theorem 3.6, implies in particular that there exists an optimal solution to $(P_{\beta,h})$ in $M_h \cap M(\Omega_o)$ which is comprised of at most $n(n+1)/2$ distinct support points.

Finally, we prove subsequential convergence of discrete optimal solutions for $h \to 0$.

Proposition 5.2. *For $h \leq h_0$ denote by $\bar{\omega}_{\beta,h}$ an arbitrary optimal solution to $(P_{\beta,h})$. There exists at least one subsequence of $\{\bar{\omega}_{\beta,h}\}_{h>0}$ (denoted in the same way), converging in the weak* topology for $h \to 0$. Every accumulation point $\bar{\omega}_\beta$ of $\{\bar{\omega}_{\beta,h}\}_{h>0}$ is a minimizer of (P_β) and*

$$\|\bar{\omega}_{\beta,h}\|_{M(\Omega_o)} \to \|\bar{\omega}_\beta\|_{M(\Omega_o)}, \quad \psi_h(\bar{\omega}_{\beta,h}) \to \psi(\bar{\omega}_\beta).$$

Furthermore, if there holds

$$\#\operatorname{supp}\bar{\omega}_{\beta,h} \leq n(n+1)/2, \quad \forall h > 0$$

then the same holds for every accumulation point.

Proof. Let $\{\bar{\omega}_{\beta,h}\}_{h>0}$ be a sequence of discrete optimal solutions and let $\bar{\omega}$ be an optimal solution to (P_β). For h sufficiently small there holds

$$\beta\|\bar{\omega}_{\beta,h}\|_{M(\Omega_o)} \leq \psi_h(\bar{\omega}_{\beta,h}) + \beta\|\bar{\omega}_{\beta,h}\|_{M(\Omega_o)} \leq \psi_h(\bar{\omega}) + \beta\|\bar{\omega}\|_{M(\Omega_o)}. \tag{5.5}$$

Due to $\mathcal{I}_h(\bar{\omega}_\beta) \to \mathcal{I}(\bar{\omega}_\beta)$ the right-hand side in this inequality is bounded independently of h. From this, we deduce the boundedness of the sequence $\{\bar{\omega}_{\beta,h}\}_{h>0}$. Thus, there exists a subsequence denoted in the same way and a measure $\bar{\omega}_\beta \in M^+(\Omega_o)$ with $\bar{\omega}_{\beta,h} \rightharpoonup^* \bar{\omega}_\beta$ for $h \to 0$. Due to the weak* lower semi-continuity of the norm and the uniform convergence of the sensitivities there holds

$$\psi(\bar{\omega}_\beta) + \beta\|\bar{\omega}_\beta\|_{M(\Omega_o)} \leq \liminf_{h\to 0}[\psi_h(\bar{\omega}_{\beta,h}) + \beta\|\bar{\omega}_{\beta,h}\|_{M(\Omega_o)}] \leq \psi(\bar{\omega}) + \beta\|\bar{\omega}\|_{M(\Omega_o)}$$

by taking the limes inferior on both sides of (5.5). Therefore $\bar{\omega}_\beta$ is also an optimal solution of (P_β) and

$$\psi_h(\bar{\omega}_{\beta,h}) + \beta\|\bar{\omega}_{\beta,h}\|_{M(\Omega_o)} \to \psi(\bar{\omega}_\beta) + \beta\|\bar{\omega}_\beta\|_{M(\Omega_o)}.$$

Furthermore, due to the weak* convergence of $\bar{\omega}_{\beta,h}$, we obtain

$$\|\bar{\omega}_{\beta,h}\|_{M(\Omega_o)} = \langle 1, \bar{\omega}_{\beta,h}\rangle \to \|\bar{\omega}_\beta\|_{M(\Omega_o)} = \langle 1, \bar{\omega}_\beta\rangle = \|\bar{\omega}_{\beta,h}\|_{M(\Omega_o)}.$$

The convergence of $\psi_h(\bar{\omega}_{\beta,h})$ is a direct consequence of the convergence of the objective function values as well as the the convergence of the norms. The result on the number of support points follows from [43, Proposition C.1], again using that $\dim \operatorname{Sym}(n) = n(n+1)/2$. □

Observe that the different implementations of Algorithms 2 presented in Section 4.1 can be directly applied to $(P_{\beta,h})$. Following Theorem 5.1 the position $\hat{x}^k$ of the new Dirac delta function can be chosen from $\mathcal{N}_h$. Therefore step 2. in Algorithm 2 amounts to the computation of the discrete gradient $\psi_h'(\omega^k)$ and the determination its maximum in $\mathcal{N}_h$. The latter one can be done efficiently by $O(\#\mathcal{N}_h)$ operations.

5.2. **Post-processing of the discrete design measure.** By Theorem 3.6 the support of an optimal design $\bar\omega_\beta$ can be limited to $n(n+1)/2$ points. In practice, this upper bound is often rather pessimistic. However, due to discretization error, the support of a discrete solution $\bar\omega_{\beta,h} \in M_h$ of $(P_{\beta,h})$ can be bigger than that of the continuous counterpart $\bar\omega_\beta$, while still respecting the upper bound $n(n+1)/2$. Usually, a sensor at a specific location in the continuous solution appears spread out over several adjacent grid points in the numerical solution. A similar effect has been observed and theoretically investigated in the context of sparse deconvolution in the presence of noise; cf. [24]. As a remedy, we employ the following heuristic post-processing of the discrete solution: First, we cluster the support of $\bar\omega_{\beta,h}$ into $N_c \leq \#\operatorname{supp}\bar\omega_{\beta,h}$ sets $S_i \subset \Omega_o$, with $\operatorname{diam}(S_i) \leq Ch$. Then, we construct a new design $\bar\omega^S = \sum_{i=1,\dots,N_c} \lambda_i^S \delta_{x_i^S}$ with $\lambda_i^S = \int_{S_i} \mathrm{d}\bar\omega_h$ summing up the coefficients of each cluster, and $x_i^S = \int_{S_i} x\,\mathrm{d}\bar\omega_h/\lambda_i^S$ the locations by the center of mass. Note that this introduces an additional error in the location of the support points of order h, which is not worse than what we can expect from $\bar\omega_h$. Additionally, the weak*-convergence result for $h \to 0$ from Proposition 5.2 is not affected by this post-processing.

5.3. **Discretization of (P_β^ε).** We briefly comment on the discretization of the regularized sub-problems (P_β^ε). We adapt the approach from [42, 18] and discretize the design by piece-wise linear finite elements on the observation set, denoted by U_h. We endow this space with the lumped inner product defined for any $\varphi, \psi \in U_h \subset C(\Omega_o)$ in the usual way as

$$(\varphi,\psi)_{\Omega_o,h} = \int_{\Omega_o} i_h(\varphi\psi)(x)\,\mathrm{d}x.$$

The approximation of (P_β^ε) is then defined as

$$\min_{\omega_h \in U_h, \omega_h \geq 0} \Big[\psi_h(\Lambda_h\omega_h) + \beta\|\omega_h\|_{L^1(\Omega_o)} + \frac{\varepsilon}{2}\|\omega_h\|^2_{L^2(\Omega_o),h}\Big], \tag{$P_{h,\beta}^\varepsilon$}$$

where $\|\omega_h\|^2_{L^2(\Omega_o),h} = (\omega_h,\omega_h)_{\Omega_o,h}$ is the lumped regularization term. Here, the appearance of $\Lambda_h\omega_h$ turns integrals involving the finite element function ω_h into appropriate lumped integrals, i.e., we obtain

$$\mathcal{I}_h(\Lambda_h\omega_h)_{ij} = (\partial_i S^h[\hat q]\partial_j S^h[\hat q], \omega_h)_h.$$

Note also that $\|\omega_h\|_{L^1(\Omega_o)} = \|\omega_h\|_{M(\Omega_o)} = \|\Lambda_h\omega_h\|_{M(\Omega_o)}$. The existence of an optimal solution to $(P_{h,\beta}^\varepsilon)$, for h small enough, can be shown by similar arguments as for the unregularized discrete problem. Additionally uniqueness of the solution follows using the strict convexity of the regularization term. The necessary and sufficient optimality conditions can be derived and are equivalent to the point-wise projection formula

$$\bar\omega_{\beta,h}^\varepsilon(x_i) = \max\left\{-\frac{1}{\varepsilon}(\psi_{l,h}'(\bar\omega_{\beta,h}^\varepsilon)(x_i) + \beta), 0\right\} \quad \forall x_i \in \mathcal{N}_h \cap \Omega_o. \tag{5.6}$$

For a discussion and comparison of different discretization schemes of the regularized problem we refer to [42, Section 4.5.3].

6. Numerical examples

We end this paper with a numerical study of two test examples. In the following we consider the unit square $\bar\Omega = \Omega_o = [0,1]^2$ and a sequence $\mathcal{T}_{h_k}$, $k \in \{1,2,\dots,9\}$, of uniform triangulations of Ω_o with $h_k = \sqrt{2}/2^k$. Our aim in this section is twofold. First, we want to numerically illustrate the theoretical results. Secondly, we want to study the practical performance of the Algorithms according to various criteria including the computational

time, the evolution of the sparsity pattern throughout the iterations and the influence of the fineness of the triangulation. In all examples we consider the A-optimal design problem, i.e. $\Psi = \operatorname{Tr}(\cdot)^{-1}$ and the discrete state and the associated sensitivities $\partial S[\hat{q}]$ are computed for a fixed $\hat{q}$ once at the beginning. During the execution of the different variants of Algorithms 2 and 3 no additional PDEs need to be solved. Moreover, the gradient of the reduced cost functional is given by

$$\left[\psi'(\omega)\right](x) = -\operatorname{Tr}(\mathcal{I}(\omega)^{-1}\,\mathcal{I}(\delta_x)\,\mathcal{I}(\omega)^{-1}) = -\|\mathcal{I}(\omega)^{-1}\partial S[\hat{q}](x)\|^2_{\mathbb{R}^n} \quad \forall x \in \Omega,$$

which relates the pointwise value of the gradient directly to the corresponding sensitivity vector $\partial S[\hat{q}](x) \in \mathbb{R}^n$. A corresponding computation on the discrete level allows for an efficient implementation based on a single Cholesky-decomposition of $\mathcal{I}(\omega)$ in each iteration. Moreover, a corresponding expression for the Hessian-vector-product $[\psi''(\omega)(\delta\omega)](x)$ for $\delta\omega \in M(\Omega)$ can be derived by differentiating the above expression. In both examples, the assumptions on the continuous and discrete state equation, see Assumption 1 and Assumption 4, respectively, can be easily verified.

6.1. **Example 1.** As a first example for the state equation (2.1), we take a convection-diffusion process where for a given $q \in Q_{ad} = \{\, q \in \mathbb{R}^3 \mid 5 \geq q_1 \geq 0.25 \,\}$ the associated state $y = S[q] \in H^1_0(\Omega) \cap C(\Omega_o)$ is the unique solution to

$$a(q,y)(\varphi) = \int_\Omega \left[q_1 \nabla y \cdot \nabla\varphi + q_2 \varphi \frac{\partial y}{\partial x_1} + q_3 \varphi \frac{\partial y}{\partial x_2} \right] \mathrm{d}x = \int_\Omega f\varphi \,\mathrm{d}x, \tag{6.1}$$

for all $\varphi \in H^1_0(\Omega)$. The forcing term f is chose as $\exp(3(x_1^2 + x_2^3))$. This corresponds to the linear elliptic equation

$$-q_1 \Delta y + \begin{pmatrix} q_2 \\ q_3 \end{pmatrix} \cdot \nabla y = f \quad \text{in } \Omega,$$

together with homogeneous Dirichlet boundary conditions on $\partial\Omega$. Here, the parameter q contains the scalar diffusion and convection coefficients of the elliptic operator. As a priori guess for the parameter we choose $\hat{q} = (3, 0.5, 0.25)^\top$. Note that while (6.1) is a linear equation, the state $y \in H^1_0(\Omega) \cap C(\Omega_o)$ depends non-linearly but differentiable on q. For each $k \in \{\, 1, 2, 3 \,\}$ the sensitivity $\delta y_k = \partial_k S[\hat{q}] \in H^1_0(\Omega) \cap C(\Omega_o)$ can be computed from (2.2). Due to the tri-linearity of the form $a(\cdot,\cdot)(\cdot)$ it fulfills

$$a(\hat{q}, \delta y_k)(\varphi) = a(\mathbf{e}_k, \hat{y})(\varphi) \quad \forall \varphi \in H^1_0(\Omega),$$

where $\hat{y} = S[\hat{q}]$ and $\mathbf{e}_k \in \mathbb{R}^3$ denotes the k-th canonical unit vector.

6.1.1. *First order optimality condition.* In this section we numerically verify the discrete first-order necessary and sufficient optimality conditions from Theorem 5.1. Therefore we compute an A-optimal design for Example 1 on grid level nine $\mathcal{T}_{h_9}$ for $\beta = 1$ and $\mathcal{I}_0 = 0$. For the computation we use Algorithm 2 (together with Algorithm 1 and a full resolution of the arising finite-dimensional subproblems), until the residual is below machine precision. We obtain a discrete optimal design $\bar{\omega}_h$ in $M^+(\Omega_o) \cap M_h$ with five support points. By closer inspection we observe that two of the computed support points are located in adjacent nodes of the triangulation. Applying the post-processing from Section 5.2, we obtain the design given in Figure 1. Alongside we plot the isolines of $-\psi'_h(\bar{\omega}_{\beta,h})$. As predicted by Theorem 5.1, $-\psi'_h(\bar{\omega}_{\beta,h})$ is bounded from above by the cost parameter $\beta = 1$ and the support points of $\bar{\omega}_{\beta,h}$ align themselves with those points in which this upper bound is achieved.

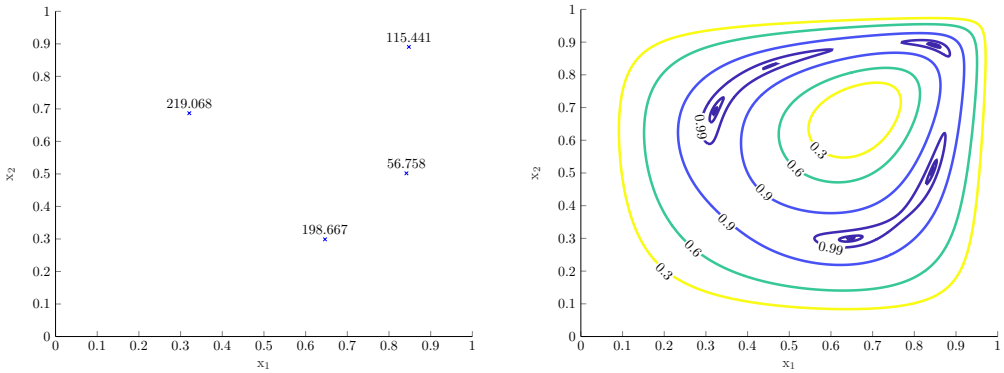

(A) Optimal design $\bar{\omega}_{\beta,h}$. (B) Isolines of $-\psi_h(\bar{\omega}_{\beta,h})$.

FIGURE 1. Optimal design and isolines of the gradient.

6.1.2. *Confidence domains of the optimal estimator.* Given the optimal design $\bar{\omega}_h$ from Figure 1a, and $K > 0$ we note that the measure $\bar{\omega}_h^K = (K/\|\bar{\omega}_{\beta,h}\|_{M(\Omega_o)})\bar{\omega}_{\beta,h}$ is an optimal solution to

$$\min_{\omega \in M^+(\Omega_o)} \operatorname{Tr}(\mathcal{I}_h(\omega_h)^{-1}) \quad \text{subject to } \|\omega_h\|_{M(\Omega_o)} \leq K,$$

since the A-optimal design criterion is positive homogeneous; see Proposition 3.9. In this section we compute the linearised confidence domains (2.8) of the least-squares estimator $\tilde{q}$ from (2.4) corresponding to $\bar{\omega}_h^K$ for $K = 3 \cdot 10^4$.

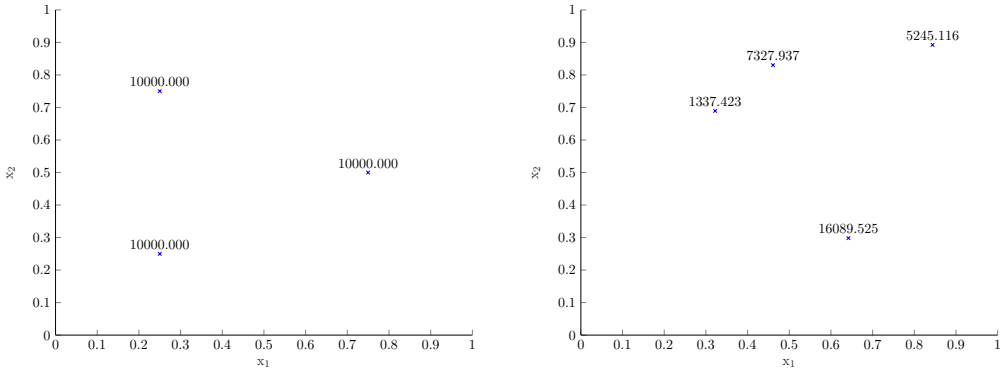

FIGURE 2. Reference measures ω_1 (left) and $\bar{\omega}_h^{K,W}$ (right).

Note that, given a sparse design measure ω, and the associated linearised estimator $\tilde{q}_{\text{lin}} = (\tilde{q}^1_{\text{lin}}, \tilde{q}^2_{\text{lin}}, \tilde{q}^3_{\text{lin}})^T$, see (2.7), there holds $\operatorname{Cov}[\tilde{q}_{\text{lin}}, \tilde{q}_{\text{lin}}] = \mathcal{I}_h(\omega)^{-1}$; see the discussion in Section 2. Consequently we have

$$\mathcal{I}_h(\omega)^{-1}_{kk} = \operatorname{Var}[\tilde{q}^k_{\text{lin}}], \ k \in \{1,2,3\} \quad \text{and} \quad \operatorname{Tr}(\mathcal{I}_h(\omega)^{-1}) = \sum_{k=1}^{3} \operatorname{Var}[\tilde{q}^k_{\text{lin}}].$$

As a comparison, we also consider the estimators corresponding to two reference designs of the same norm. The first measure ω_1 is chosen as a linear combination of three Dirac delta

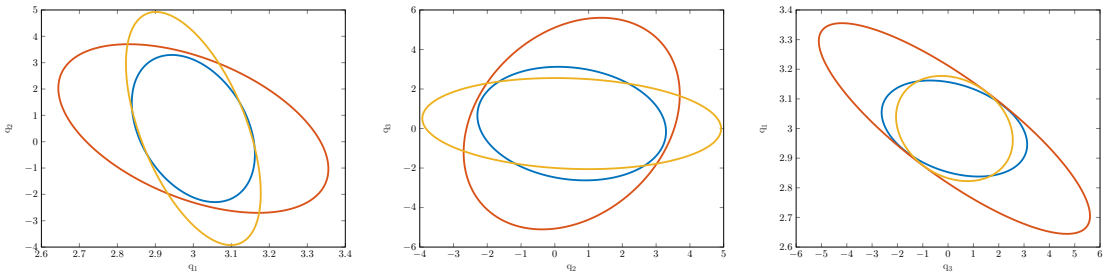

(A) Ellipsoids for $(q_1, q_2)^T$. (B) Ellipsoids for $(q_2, q_3)^T$. (C) Ellipsoids for $(q_3, q_1)^T$.

FIGURE 3. Confidence ellipsoids for the estimators associated to $\bar{\omega}_h^K$ (blue), ω_1 (red) and $\bar{\omega}_h^{K,W}$ (yellow).

functions with equal coefficients while the second measure $\bar{\omega}_h^{K,W}$ is a solution to

$$\min_{\omega \in M^+(\Omega_o)} \operatorname{Tr}(W\, \mathcal{I}_h(\omega_h)^{-1} W) \quad \text{subject to } \|\omega_h\|_{M(\Omega_o)} \leq K, \tag{6.2}$$

where $W = \operatorname{diag}(1, 1, 4)$, i.e. we place more weight on the variance for the estimation of q_3. The designs ω_1 and $\bar{\omega}_h^{K,W}$ are depicted in Figure 2.

For a better visualization we plot the 50%-linearised confidence domains of the obtained estimators for the two dimensional parameter vectors $(q_1, q_2)^T$, $(q_2, q_3)^T$, and $(q_3, q_1)^T$ in Figure 3. Additionally, for each design we report $\operatorname{Tr}(\mathcal{I}_h(\omega)^{-1})$ as well as the diagonal entries of $\mathcal{I}_h(\omega)^{-1}$ in Table 1. As expected, since $\bar{\omega}_{\beta,h}$ is chosen by the A-optimal design criterion,

TABLE 1. Trace and diagonal entries of $\mathcal{I}_h(\omega)^{-1}$

ω	$\mathcal{I}_h(\omega)^{-1}_{11}$	$\mathcal{I}_h(\omega)^{-1}_{22}$	$\mathcal{I}_h(\omega)^{-1}_{33}$	$\operatorname{Tr}(\mathcal{I}_h(\omega)^{-1})$
$\bar{\omega}_h^K$	0.019	5.627	5.955	11.601
ω_1	0.091	7.388	20.678	28.157
ω_2	0.023	14.12	3.831	17.974

we observe that

$$\operatorname{Tr}(\mathcal{I}_h(\bar{\omega}_h^K)^{-1}) \leq \operatorname{Tr}(\mathcal{I}_h(\omega_2)^{-1}) \leq \operatorname{Tr}(\mathcal{I}_h(\omega_1)^{-1}). \tag{6.3}$$

Moreover we note that $\mathcal{I}_h(\bar{\omega}_h^K)^{-1}_{kk} < \mathcal{I}_h(\omega_1)^{-1}_{kk}$ for all k, i.e. the optimal estimator estimates all unknown parameters with a smaller variance than the estimator associated to the reference design ω_1. As a consequence, the linearised confidence domains of the optimal estimator are contained in those of the one corresponding to ω_1; see Figure 3. In contrast, considering ω_2, we have $\mathcal{I}_h(\omega_2)^{-1}_{33} < \mathcal{I}_h(\bar{\omega}_h^K)^{-1}_{33}$ and $\mathcal{I}_h(\bar{\omega}_h^K)^{-1}_{kk} < \mathcal{I}_h(\omega_2)^{-1}_{kk}$ for $k = 1, 2$, i.e. the third parameter is estimated more accurately by choosing the measurement locations and weights according to ω_2 while the variance for the estimation of the other parameters is larger. This is a consequence of the different weighting of the matrix entries in (6.3). On the one hand, the obtained results show the efficiency of an optimally chosen measurement design at least for the linearised model. On the other hand, they also highlight that the properties of the obtained optimal estimators crucially depend on the choice of the optimal design criterion Ψ.

6.1.3. *Comparison of point insertion algorithms.* In this section we investigate the performance of the successive point insertion algorithm presented in Section 4.1. We consider the same setup as in Section 6.1.1, i.e. we solve the A-optimal design problem for Example 1 on grid level nine with $\beta = 1$ and $\mathcal{I}_0 = 0$. The step size parameters α and γ in (4.4) are both chosen as $1/2$ throughout the experiments and the iteration is terminated if either $\Phi(\omega^k) \leq 10^{-9}$ or if the iteration number k exceeds $2 \cdot 10^4$. The aim of this section is to confirm the theoretical convergence results for Algorithm 2 and to demonstrate the necessity of additional point removal steps. Additionally we want to highlight the differences between the three presented choices of the new coefficient vector λ^{k+1} concerning the sparsity of the iterates and the practically achieved acceleration of the convergence. Specifically, we consider the following implementations of step 4. in Algorithm 2:

GCG: In the straightforward implementation of the GCG algorithm we set $\lambda^{k+1} = \lambda^{k+1/2}$, i.e. only steps 1. to 4. are performed.

SPINAT: Here, we employ the procedure suggested in [16], termed "Sequential Point Insertion and Thresholding". In step 5., λ^{k+1} is determined from a proximal gradient iteration (4.14). The step size is chosen as $\sigma_k = (1/2)^n \sigma_{0,k}$, where $\sigma_{0,k} > 0$ for the smallest $n \in \mathbb{N}$ giving $F(\omega(\lambda^{k+1}(\sigma_k))) \leq F(\omega(\lambda^{k+1/2}))$. In particular, given $\omega^{k+1/2} = \sum_i \lambda_i^{k+1/2} \delta_{x_i}$, we choose $\sigma_{0,k}$ as

$$\sigma_{0,k} = \max\left\{100, -2 \min_i \left\{ \frac{\lambda_i}{-\psi'(\omega^{k+1/2})(x_i) - \beta} \right\} \right\}.$$

Note that by this choice of $\sigma_{0,k}$, the coefficients of all points $x \in \operatorname{supp} \omega^{k+1/2}$ with $-\psi'(\omega^{k+1/2})(x) < \beta$ are set to zero in the first trial step (i.e. for $n = 0$).

PDAP: Here, the coefficient vector λ^{k+1} is chosen as in (4.15) by solving the finite dimensional sub-problem (4.13) up to machine precision in each iteration. For the solution we use a semi-smooth Newton method with a globalization strategy based on a backtracking line-search. The convergence criterion for the solution of the sub-problems is based on the norm of the Newton-residual. Since, this method can be interpreted as a method operating on a set of active points $\mathcal{A}_k = \operatorname{supp} \omega^k$ (see section 4.2), we reference it by the name: "Primal-Dual Active Point".

All three versions of the algorithm are also considered with an application of the sparsification step in Algorithm 1 at the end of each iteration. In the following this will be denoted by an additional "+PP".

In Figure 4a we plot the residual $r_F(\omega^k)$ for all considered algorithms over the iteration counter k. For GCG as well as SPINAT we observe a rapid decay of the computed residuals in the first few iterations. However, asymptotically both admit a sub-linear convergence rate, suggesting that the convergence result derived in Theorem 4.6 is sharp in this instance. The additional application of Algorithm 1 has no significant impact on the convergence behavior. We additionally note that both GCG and SPINAT terminate only since the maximum number of iterations is exceeded while the computed residuals $r_F(\omega^k)$ and thus also the primal-dual gap $\Phi(\omega^k)$ remain above 10^{-3}. In contrast, PDAP terminates after few iterations within the tolerance. The results clearly indicate a better convergence rate than the one derived in Theorem 4.6.

Next, we study the influence of the different point removal steps on the sparsity pattern of the obtained iterates in Figure 4b. For GCG we notice that the number of support points increases monotonically up to approximately 60. This suggests a strong clusterization of the intermediate support points around those of $\bar{\omega}_{\beta,h}$ which is possibly caused by the small curvature of $-\psi_h'(\bar{\omega}_{\beta,h})$ (see Figure 1b) in the vicinity of its global maxima. A similar

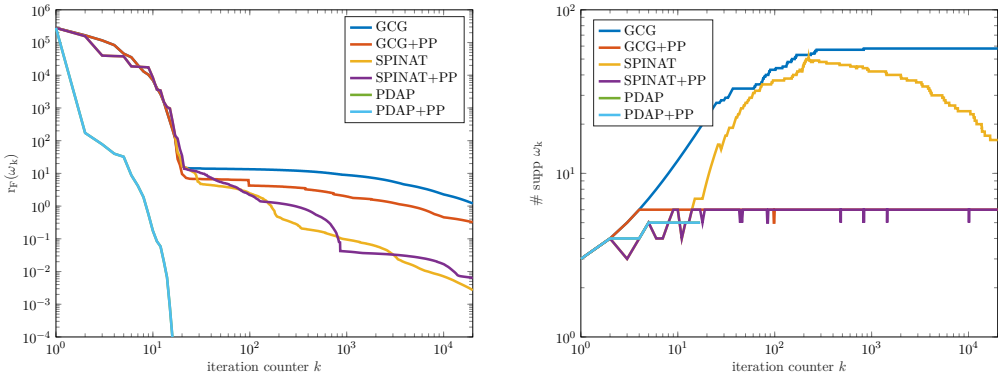

(A) Residual $r_F(\omega^k)$ over k. (B) Support size $\#\operatorname{supp}\omega^k$ over k.

FIGURE 4. Residual and support size plotted over iteration number k.

behavior can be observed for the iterates obtained through SPINAT. However, compared to GCG the support size grows slower due to the additional projected gradient step in every iteration. Additionally, after reaching a threshold at approximately $k = 110$, the support size decreases monotonically in the remaining iterations. Concerning the application of Algorithm 1, we observe that the support remains bounded by $6 = 3(3+1)/2$ as predicted by Proposition 4.7. We note that this upper bound is achieved in almost all but the first few iterations for GCG and SPINAT. In contrast, PDAP yields iterates comprising less than six support points independently of the additional post-processing. A closer inspection reveals that the loop in Algorithm 1 is not carried out in any iteration, i.e. the sparsity of the iterates is fully provided by the exact solution of the finite-dimensional sub-problems.

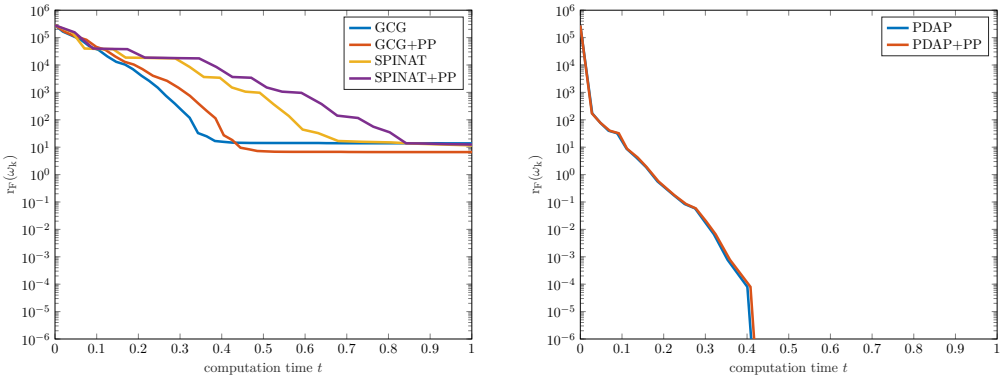

(A) Residual for GCG and SPINAT. (B) Residual for PDAP.

FIGURE 5. Residual $r_F(\omega^k)$ plotted over the first second of the running time.

Last, we report on the computational time for the setup considered before, in order to account for the numerical effort of the additional point removal steps. The evolution of the residuals in the first second of the running time for GCG and SPINAT can be found in Figure 5a. We observe that neither the additional projected gradient steps nor the additional application of Algorithm 1 lead to a significant increase of the computational time. For PDAP, the measurement times and residuals for all iterations are shown in Figure 5b. We point out that PDAP converges after 12 iterations computed in approximately 0.4 seconds

in this example. This is comparable to the elapsed computation time for computing 25 iterations of the GCG method. The small average time for a single iteration of PDAP is on the one hand a consequence of the uniformly bounded, low dimension of the sub-problem (4.15). On the other hand, using the intermediate iterate $\omega^{k+1/2}$ to warm-start the semi-smooth Newton method greatly benefits its convergence behavior, restricting the additional numerical effort in of PDAP in comparison to GCG to the solution of a few low-dimensional Newton systems in each iteration. These results again underline the practical efficiency of the presented acceleration strategies.

6.1.4. *Mesh-independence.* To finish our numerical studies on Example 1 we examine the influence of the mesh-size h on the performance of Algorithm 2. We again consider the A-optimal design problem for $\beta = 1$ and $\mathcal{I}_0 = 0$ on consecutively refined meshes $\mathcal{T}_{h_l}$, $l = 5, \dots, 9$. On each refinement level l the optimal design problem is solved using GCG and PDAP, respectively. The computed residuals are shown in Figure 6. For both versions we observe that the convergence rate of the objective function value is stable with respect to mesh-refinement. We point out that this indicates a better convergence behavior of PDAP also on the continuous level. A theoretical investigation of this improved rate is beyond the scope of this work but will be given in a future manuscript. Additionally, in Figure 7,

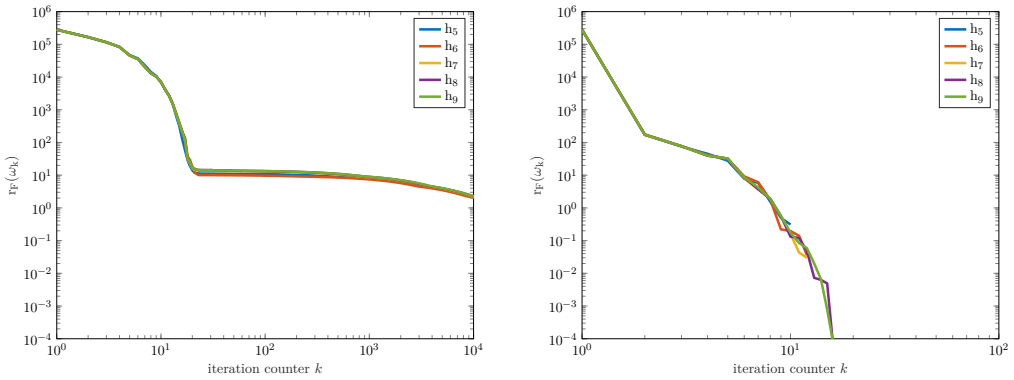

(A) Residuals for GCG. (B) Residuals for PDAP.

FIGURE 6. Evolution of residuals $r_F(\omega^k)$ over iterations k on different refinement levels.

we plot the support size over the iteration counter for each refinement level. For GCG we observe a monotonic growth of the support size up to a certain threshold. Note that the upper bound on the support size seems to depend on the spatial discretization: the finer the grid, the more clusterization around the true support points can be observed. In contrast, for PDAP, the evolution of the support size admits a mesh-independent behavior in this example.

6.2. **Example 2.** Secondly, we compare the performance of the successive point insertion algorithm and the path-following Algorithm presented in Section 4.4. Since the practical performance is aided by the low number of parameters in the previous example, we construct an example with a variable number of parameters.

The setting is motivated by the task of estimating spatially varying diffusion parameters, which is a common problem in, e.g., geophysical applications. Therefore we consider a stationary diffusion process, where the unknown parameter q is the diffusion coefficient. We

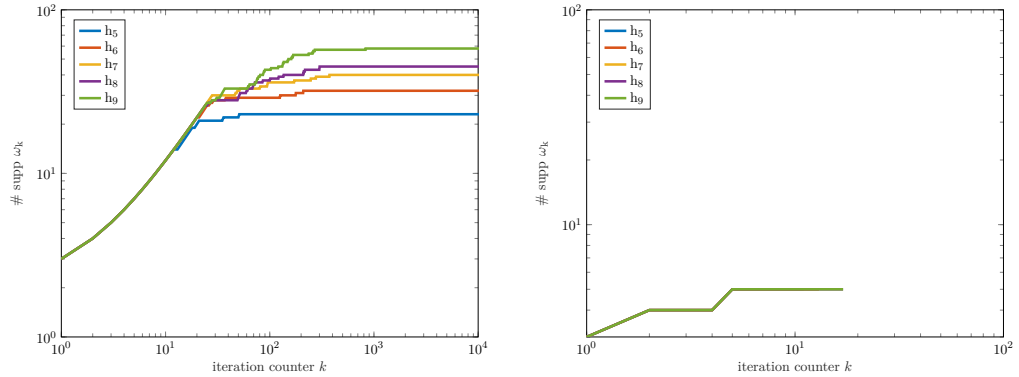

(A) $\#\operatorname{supp}\omega^k$ over k for GCG. (B) $\#\operatorname{supp}\omega^k$ over k for PDAP.

FIGURE 7. Evolution of the support size on different refinement levels.

set $\Omega = [0,1]^2$ to be the unit square and define the Dirichlet boundary as $\Gamma_D = \{0,1\}\times(0,1)$ (corresponding to the left and right boundaries). Then we define the solution space

$$Y = \left\{ \varphi \in H^1(\Omega) \;\middle|\; \varphi_{|\Gamma_D} = 0 \right\},$$

and the function $\hat{y}(x_1,x_2) = x_1$ encoding the Dirichlet data. For $q \in \mathbb{R}^n \simeq \mathbb{R}^{N\times N}$ for some $N \in \mathbb{N}$ we set

$$m[q](x) = \sum_{i=1}^{N}\sum_{j=1}^{N} q_{(i,j)}\phi_{(i,j)}, \quad \text{where } \phi_{(i,j)}(x_1,x_2) = \sin(\pi i x_1)\sin(\pi j x_2).$$

Given $q \in \mathbb{R}^{N\times N}$ the associated state $y = S[q]$ is the unique element of $\hat{Y} = \hat{y} + Y$ satisfying

$$a(q,y)(\varphi) = \int_\Omega \exp(m[q])\nabla y \cdot \nabla\varphi \,\mathrm{d}x = 0 \quad \forall \varphi \in Y. \tag{6.4}$$

It can be easily seen that (6.4) corresponds to the linear equation

$$\begin{aligned} -\nabla\cdot(\exp(m[q])\nabla y) &= 0 && \text{in } \Omega,\\ y &= x_1 && \text{on } \Gamma_D,\\ \exp(m[q])\partial_n y &= 0 && \text{on } \partial\Omega\setminus\Gamma_D. \end{aligned} \tag{6.5}$$

Note that due to the linearity of the equation, the sensitivity $\delta y_{(i,j)} = \partial_{(i,j)} S[q] \in Y$ with respect to the (i,j)-th entry of q for $i,j \in \{1,\dots,N\}$ defined in (2.2) satisfies

$$a(q,\delta y_{(i,j)})(\varphi) = -\int_{\Omega_o} \phi_{(i,j)} \exp(m[q])\,\nabla y\cdot\nabla\varphi \,\mathrm{d}x \quad \forall\varphi\in Y.$$

6.2.1. *Comparison of point-insertion and path-following: No a priori knowledge.* In this section we compare the performance of the proposed successive point-insertion (Algorithm 2) and the algorithmic solution approach based on the Hilbert-space regularization (Algorithm 3). Since both algorithms are fundamentally different and partly rely on different computational routines, a comparison in terms of number of steps is difficult. For this reason, we focus on the computation times in the following. We place special emphasis on the qualitative influence of the mesh width and the support size of the optimal design.

Therefore we consider the A-optimal design problem for Example 2 with different $N \in \mathbb{N}$ and on different refinement levels of the spatial discretization. The cost parameter is chosen as $\beta = 1$ and no a priori knowledge is assumed, i.e. $\mathcal{I}_0^N = 0$. The parameter-to-state

mapping is linearised at $\hat{q} = 0 \in \mathbb{R}^{N\times N}$. Given a fixed $N \in \mathbb{N}$ and h small enough such that the semi-discrete design problem $(P_{\beta,h})$ admits an optimal solution $\bar{\omega}^N_{\beta,h}$ we note that $\#\operatorname{supp}\bar{\omega}^N_{\beta,h} \geq n = N^2$; cf. Proposition 3.3. Consequently, by increasing N we also raise the number of optimal Dirac delta functions that both algorithms have to identify.

Concerning the different implementations of the point insertion algorithm we will restrict ourselves to PDAP as described in Section 6.1.1 without the additional application of Algorithm 1 in every iteration. As in the previous example the iteration is stopped at step k if $\Phi(\omega^k) \leq 10^{-9}$. For Algorithm 3 we set $\varepsilon_1 = 10^{-3}$ and $\varepsilon_l = \varepsilon_{l-1}/\sqrt{10}$ for $l > 1$. For each l the regularized sub-problem $(P^{\varepsilon}_{h,\beta})$ is solved by using the semi-smooth Newton method presented in [42]. We include a globalization strategy based on a damping of the Newton steps to ensure a decrease of the regularized objective function value in every iteration. The arising linear systems are solved by a cg-method up to machine precision. If the norm of the right-hand side in the Newton system is smaller than some tolerance, ε_l is decreased as described above. For a relevant comparison, we compute the residual at the end of each iteration in PDAP and at the end of each step in the semi-smooth Newton method for $(P^{\varepsilon_l}_{h,\beta})$, where $l = 1, \dots, l_{\max}$. Note that, as for the previous example, we only take the computational time for the iterations of each Algorithms into account; the state and sensitivity equations are solved beforehand.

In the following we choose $N \in \{\,5, 15\,\}$ and consider the discretized design problems $(P_{\beta,h})$ and $(P^{\varepsilon}_{h,\beta})$ on grid $\mathcal{T}_{h_k}$ for levels $k \in \{\,5, 8\,\}$. Since $0 \notin \operatorname{supp}\psi$ we construct an initial iterate different from zero. To account for the different regularities of the solutions of (P_β) and $(P^{\varepsilon}_{\beta})$, we choose the initial iterate ω^1 for the solution of $(P_{\beta,h})$ as a linear combination of $(N+1)^2$ Dirac delta functions (located in nodes of the coarse grid) while the starting point $\bar{\omega}^1_{\varepsilon} \in U_h \subset L^2(\Omega_o)$ for the solution of $(P^{\varepsilon_1}_{\beta,h})$ is chosen as $\bar{\omega}^1_{\varepsilon} \equiv 1$. Observe that $r_F(\bar{\omega}^1_{\varepsilon}) \neq r_F(\omega^1)$. However, we stress that we are interested in a qualitative comparison of both algorithms rather than a quantitative one. The results can be found in Figure 8. First, we note that the runtime for both algorithms is affected by the increased number of support points for larger N. In fact, on grid level eight, we obtain $\#\operatorname{supp}\bar{\omega}^N_{\beta,h} = 58$ for $N = 5$ and $\#\operatorname{supp}\bar{\omega}^N_{\beta,h} = 630$ for $N = 15$, respectively. Clustering adjacent support points as described in section 5.2, we obtain 30 and 240 clusters, respectively, and the post-processed solutions (as described in section 5.2) are given in Figure 9. On both grid levels we observe that the computation time for PDAP is affected more than the one for Algorithm 3 by the increased support size of the optimal design. This is a consequence of the different update strategies for the iterates in both algorithms. In each semi-smooth Newton step in Algorithm 3 the current iterate is updated globally on Ω_o. In contrast, at most one new support point is added in each iteration of PDAP. Hence, if the support of the optimal solution is increased, so is the number of necessary iterations in PDAP, explaining the increase of the computation time.

Let us now consider the influence of the number of grid points of the spatial discretization. Here, we observe that the path-following algorithm is affected more, which can be explained as follows: for each $\varepsilon > 0$ the unique optimal solution to $(P^{\varepsilon}_{h,\beta})$ is given by the component-wise projection formula (5.6). This indicates that the set of nodes in the support of the solution depends on the fineness of the discretization. As a consequence, the path-following method can only exploit the increased sparsity in later iterations (for smaller ε), which leads to larger computational times on finer grids. In contrast, in PDAP we only need to calculate the gradient $\psi'_h(\omega^k)$ as well as its maximum on the whole domain, while the dimension of the occurring sub-problems and thus also the size of the linear systems in

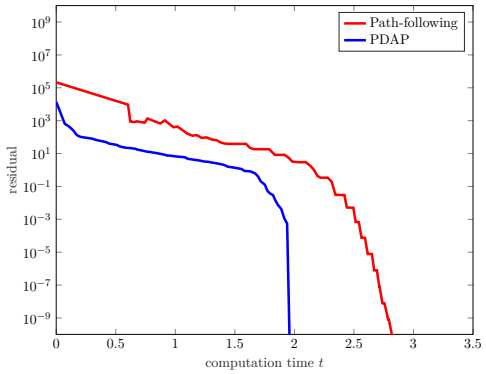

(A) Residual for $N = 5$ on grid level five.

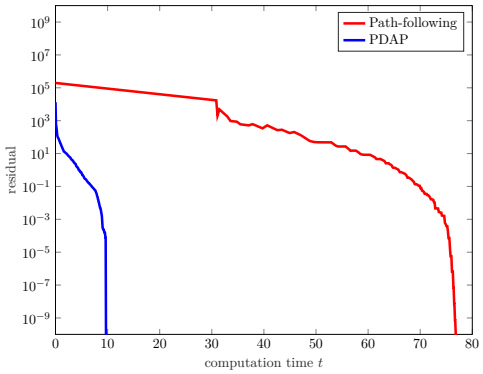

(B) Residual for $N = 5$ on grid level eight.

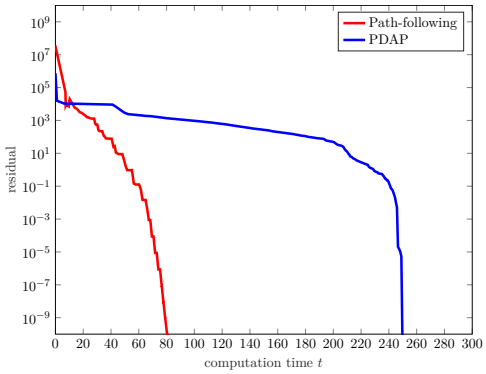

(C) Residual for $N = 15$ on grid level five.

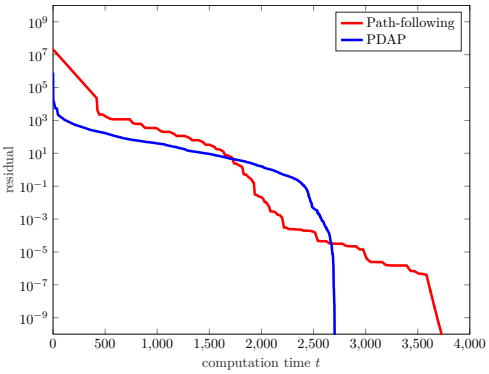

(D) Residual for $N = 15$ on grid level eight.

FIGURE 8. Residuals $r_F(\cdot)$ for various number of parameters and discretizations plotted over computation time t in seconds for $\mathcal{I}_0^N = 0$.

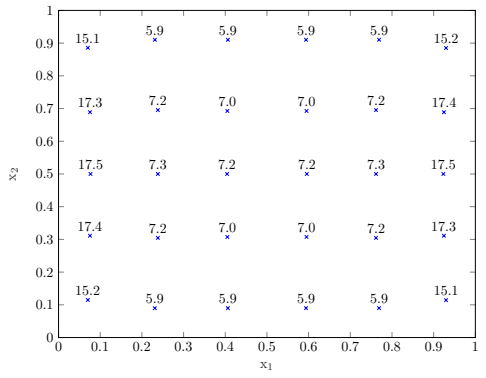

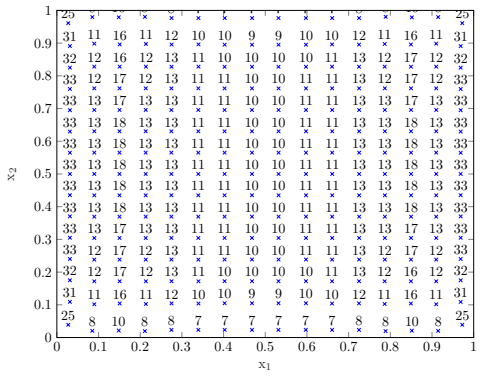

FIGURE 9. Optimal designs for $\mathcal{I}_0^N = 0$ and $N = 5$ (left) and $N = 15$ (right) on grid level eight.

the semi-smooth Newton method can be bounded independent of the discretization in every iteration. Together with the mesh-independence observations for the residual and the support size from Section 6.1.4 this explains the better scaling of the successive point insertion algorithm with respect to the number of nodes in the triangulation.

6.2.2. *Comparison of point-insertion and path-following: A priori knowledge.* To conclude this section, we consider the previous setup with incorporated a priori knowledge. Concretely, we choose $\mathcal{I}_0^N \in \mathrm{PD}(N^2)$ as a diagonal matrix where the entries on the main diagonal are given by

$$\left[\mathcal{I}_0^N\right]_{k,k} = \alpha \left(\lambda_{(i,j)} + 10\right)^2, \quad k = N(i-1)+j, \;\; i,j \in \{1,\dots N\}, \tag{6.6}$$

where $\lambda_{(i,j)} = \pi^2(i^2+j^2)$ is an eigenvalue of the Dirichlet Laplacian for the corresponding eigenfunction $\phi_{(i,j)}$ as given above (with norm $\|\phi_{(i,j)}\|_{L^2(\Omega)} = 1/2$). This choice of $\mathcal{I}_0$ corresponds to a Bayesian optimal design (for the linearized problem), where the a priori knowledge is described by a Gaussian random field on $L^2(\Omega)$ with expectation $\hat{q}$ and covariance operator $2\alpha^{-1}(-\Delta + 10\,\mathrm{Id})^{-2}$; see, e.g, [2]. In this context, the function $m[q]$ can be interpreted as a truncated Karhunen-Loève expansion corresponding to the Bayesian prior.

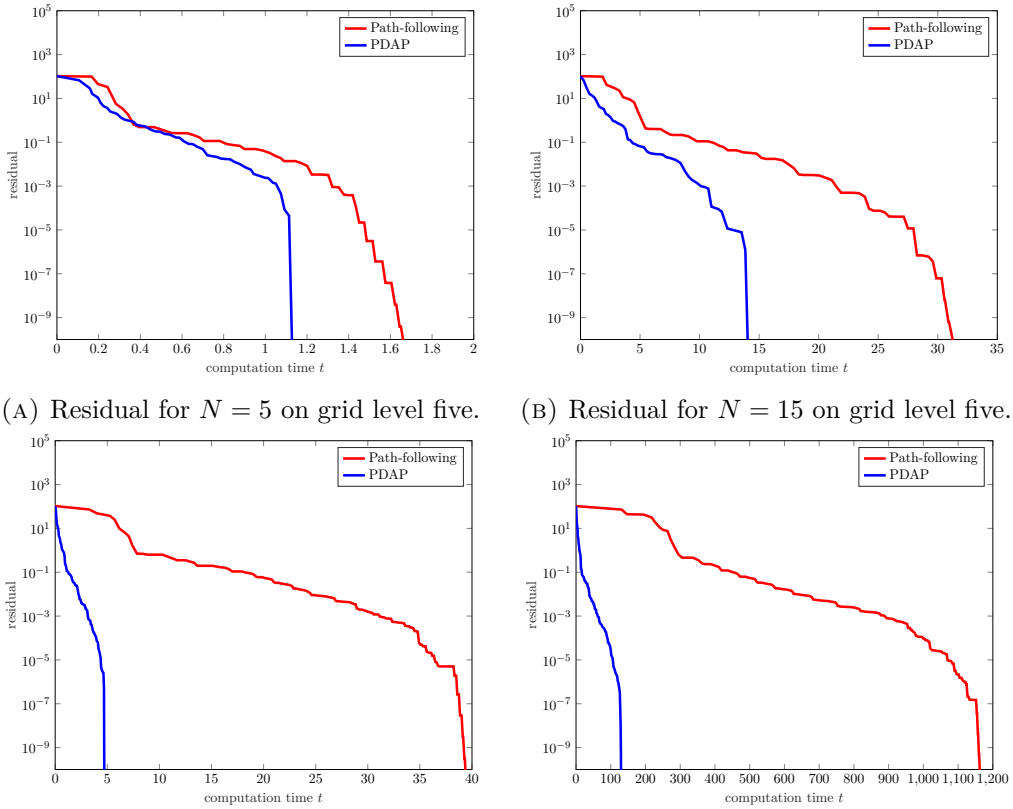

(A) Residual for $N = 5$ on grid level five. (B) Residual for $N = 15$ on grid level five.

(C) Residual for $N = 5$ on grid level eight. (D) Residual for $N = 15$ on grid level eight.

FIGURE 10. Residual $r_F(\cdot)$ for different N and discretizations plotted over computation time t in seconds for $\mathcal{I}_0^N$ given by the prior (6.6) with $\alpha = 10^{-5}$.

Since $\mathcal{I}_0$ is positive definite we can choose the starting point for both algorithms as $\omega^1 = 0$. In Figure 10 the computed residuals for the path-following algorithm and PDAP are shown for $\alpha = 10^{-5}$. For the path-following algorithm we again observe an increased computation time with respect to the spatial discretization in comparison to PDAP. Due to the positive definite $\mathcal{I}_0$, the support of the solution is not bounded from below by $n = N^2$. Concretely,

on grid level eight there holds $\#\operatorname{supp}\bar{\omega}^N_{\beta,h} = 26$ for $N = 5$ and $\#\operatorname{supp}\bar{\omega}^N_{\beta,h} = 38$ for $N = 15$, i.e. the number of optimal Dirac delta functions does not increase as significantly as in the case of $\mathcal{I}_0 = 0$ for larger N. Consequently, we also observe a better behavior of the computation time for PDAP with respect to N. The corresponding optimal designs can be found in Figure 11. As in the first example, the displayed designs are obtained by the post-processing procedure described in Section 5.2, which leads to 10 and 18 connected clusters of the support for $N = 5$ and $N = 10$, respectively.

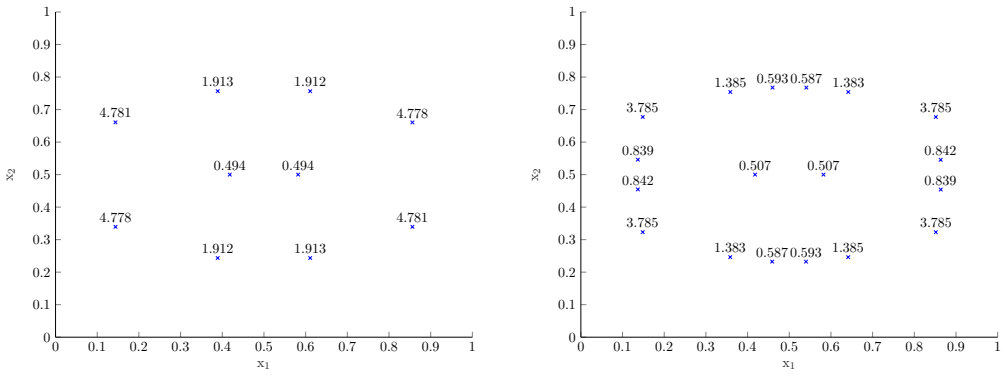

FIGURE 11. Optimal designs for $\mathcal{I}_0^N$ given by the prior (6.6) with $\alpha = 10^{-5}$ and $N = 5$ (left) and $N = 15$ (right) on grid level eight.

6.2.3. *Further acceleration strategies.* In the previous sections we observed that PDAP scales well with respect to the spatial discretization while it does not scale well with respect to the support size of the optimal design. As discussed earlier, this is mainly caused by inserting only one point in every iteration. To remedy this, we propose a heuristic acceleration strategy. From Remark 4 we know that the convergence results from Theorem 4.6 hold for PDAP if we choose the intermediate iterate as $\omega^{k+1/2} = \omega^k + v^k$, where $v^k \in M(\Omega_o)$ is chosen such that $\hat{x}^k \cup \operatorname{supp}\omega^1 \subset \operatorname{supp}\omega^{k+1/2}$. Additionally, we recall that every optimal design $\bar{\omega}^N_{\beta,h}$ fulfills the support condition (3.5). We therefore choose $v^k = -(M_0/\beta)\psi_h'\delta_{\hat{x}^k} + \tilde{v}^k$, where $\hat{x}^k \in \arg\min_{\Omega_o}\psi_h'(\omega^k)$ and $\tilde{v}^k$ is a positive linear combination of Dirac delta functions corresponding to sufficiently large local maxima of $-\psi_h'(\omega^k)$. In more detail, we set

$$\tilde{v}^k \in \left\{ \sum_{i=1}^{m} -\frac{M_0}{\beta}\psi_h'(\omega^k)(x_i)\delta_{x_i} \;\middle|\; x_i \text{ is local maximum of } -\psi_h(\omega^k),\ -\psi_h(\omega^k)(x_i) > \beta \right\}$$

such that $\#\operatorname{supp} v^k \leq n(n+1)/2$. This ensures that the dimension of the sub-problems in PDAP stays uniformly bounded throughout the iterations. However, we note that in our numerical experiments this upper bound on the support of v^k was never attained. The resulting algorithm will be referenced as Multi-PDAP in the following.

To compare the three algorithms we again consider the A-optimal design problem for Example 2 on $\mathcal{T}_{h_8}$ with $N \in \{5, 15\}$. The cost parameter and a priori knowledge are chosen as $\beta = 1$ and $\mathcal{I}_0 = 0$, respectively. The computed residuals over the computation time are plotted in Figure 12. We observe that the insertion of multiple points in each iteration significantly improves the speed of convergence of the successive point insertion algorithm, which shows the practical efficiency of the proposed heuristic strategy. Finally, we again stress that all comparisons between the two implementations of PDAP and Algorithm 3

should not be understood quantitatively; the path-following algorithm may possibly be accelerated by, e.g., the inexact solution of the regularized sub-problems.

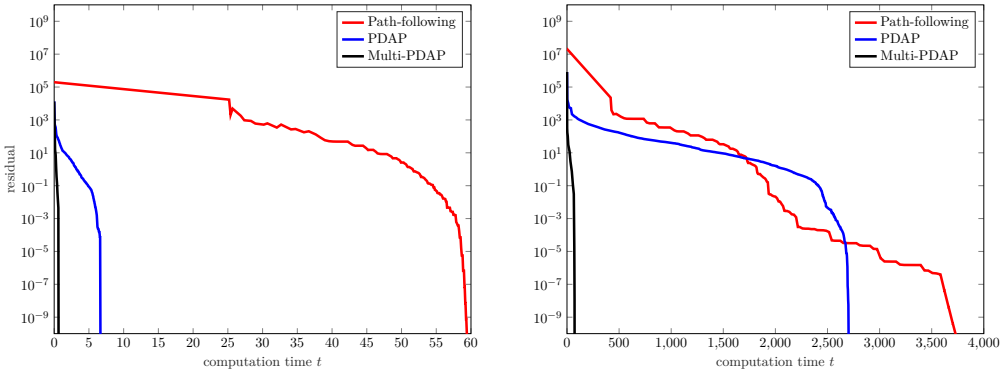

(A) Residual for $N = 5$ on level eight. (B) Residual for $N = 15$ on level eight.

FIGURE 12. Evolution of the residual $r_F(\cdot)$ over the computation time t in seconds on grid level eight for different numbers of parameters.

ACKNOWLEDGEMENTS

K. Pieper acknowledges funding by the US Department of Energy Office of Science grant DE-SC0016591 and by the US Air Force Office of Scientific Research grant FA9550-15-1-0001. D. Walter acknowledges support by the DFG through the International Research Training Group IGDK 1754 "Optimization and Numerical Analysis for Partial Differential Equations with Nonsmooth Structures". Furthermore, support from the TopMath Graduate Center of TUM Graduate School at Technische Universität München, Germany and from the TopMath Program at the Elite Network of Bavaria is gratefully acknowledged.

REFERENCES

[1] R. A. ADAMS, *Sobolev spaces*, Pure and applied mathematics, Academic Press, New York, 1978.
[2] A. ALEXANDERIAN, N. PETRA, G. STADLER, AND O. GHATTAS, *A-optimal design of experiments for infinite-dimensional Bayesian linear inverse problems with regularized ℓ_0-sparsification*, SIAM J. Sci. Comput., 36 (2014), pp. A2122–A2148.
[3] A. C. ATKINSON, A. N. DONEV, AND R. D. TOBIAS, *Optimum experimental designs, with SAS*, vol. 34 of Oxford Statistical Science Series, Oxford University Press, Oxford, 2007.
[4] C. L. ATWOOD, *Sequences converging to D-optimal designs of experiments*, Ann. Statist., 1 (1973), pp. 342–352.
[5] M. AVERY, H. T. BANKS, K. BASU, Y. CHENG, E. EAGER, S. KHASAWINAH, L. POTTER, AND K. L. REHM, *Experimental design and inverse problems in plant biological modeling*, J. Inverse Ill-Posed Probl., 20 (2012), pp. 169–191.
[6] H. T. BANKS AND K. L. REHM, *Experimental design for vector output systems*, Inverse Probl. Sci. Eng., 22 (2014), pp. 557–590.
[7] D. M. BATES AND D. G. WATTS, *Nonlinear regression analysis and its applications*, Wiley Series in Probability and Mathematical Statistics: Applied Probability and Statistics, John Wiley & Sons, Inc., New York, 1988.
[8] I. BAUER, H. G. BOCK, S. KÖRKEL, AND J. P. SCHLÖDER, *Numerical methods for optimum experimental design in DAE systems*, J. Comput. Appl. Math., 120 (2000), pp. 1–25. SQP-based direct discretization methods for practical optimal control problems.
[9] E. M. L. BEALE, *Confidence regions in non-linear estimation*, J. Roy. Statist. Soc. Ser. B, 22 (1960), pp. 41–88.

[10] R. Becker, M. Braack, and B. Vexler, *Parameter identification for chemical models in combustion problems*, Appl. Numer. Math., 54 (2005), pp. 519–536.
[11] H. G. Bock, *Randwertproblemmethoden zur Parameteridentifizierung in Systemen nichtlinearer Differentialgleichungen*, vol. 183 of Bonner Mathematische Schriften [Bonn Mathematical Publications], Universität Bonn, Mathematisches Institut, Bonn, 1987. Dissertation, Rheinische Friedrich-Wilhelms-Universität, Bonn, 1985.
[12] J. F. Bonnans and A. Shapiro, *Perturbation analysis of optimization problems*, Springer Series in Operations Research, Springer-Verlag, New York, 2000.
[13] N. Boyd, G. Schiebinger, and B. Recht, *The alternating descent conditional gradient method for sparse inverse problems*, SIAM J. Optim., 27 (2017), pp. 616–639.
[14] S. Boyd and L. Vandenberghe, *Convex optimization*, Cambridge University Press, Cambridge, 2004.
[15] K. Bredies, D. A. Lorenz, and P. Maass, *A generalized conditional gradient method and its connection to an iterative shrinkage method*, Comput. Optim. Appl., 42 (2009), pp. 173–193.
[16] K. Bredies and H. K. Pikkarainen, *Inverse problems in spaces of measures*, ESAIM Control Optim. Calc. Var., 19 (2013), pp. 190–218.
[17] E. Casas, C. Clason, and K. Kunisch, *Approximation of elliptic control problems in measure spaces with sparse solutions*, SIAM J. Control Optim., 50 (2012), pp. 1735–1752.
[18] E. Casas, R. Herzog, and G. Wachsmuth, *Approximation of sparse controls in semilinear equations by piecewise linear functions*, Numer. Math., 122 (2012), pp. 645–669.
[19] ———, *Optimality conditions and error analysis of semilinear elliptic control problems with L^1 cost functional*, SIAM J. Optim., 22 (2012), pp. 795–820.
[20] M. Chung and E. Haber, *Experimental design for biological systems*, SIAM J. Control Optim., 50 (2012), pp. 471–489.
[21] C. Clason and K. Kunisch, *A duality-based approach to elliptic control problems in non-reflexive Banach spaces*, ESAIM Control Optim. Calc. Var., 17 (2011), pp. 243–266.
[22] J. C. Dunn, *Rates of convergence for conditional gradient algorithms near singular and nonsingular extremals*, SIAM J. Control Optim., 17 (1979), pp. 187–211.
[23] ———, *Convergence rates for conditional gradient sequences generated by implicit step length rules*, SIAM J. Control Optim., 18 (1980), pp. 473–487.
[24] V. Duval and G. Peyré, *Exact support recovery for sparse spikes deconvolution*, Found. Comput. Math., 15 (2015), pp. 1315–1355.
[25] J. Elstrodt, *Maß- und Integrationstheorie*, Springer-Lehrbuch, Springer Berlin Heidelberg, 2013.
[26] V. V. Fedorov, *Theory of optimal experiments*, Academic Press, New York-London, 1972. Translated from the Russian and edited by W. J. Studden and E. M. Klimko, Probability and Mathematical Statistics, No. 12.
[27] V. V. Fedorov and P. Hackl, *Model-oriented design of experiments*, vol. 125 of Lecture Notes in Statistics, Springer-Verlag, New York, 1997.
[28] V. V. Fedorov and S. L. Leonov, *Optimal design for nonlinear response models*, Chapman & Hall/CRC Biostatistics Series, CRC Press, Boca Raton, FL, 2014.
[29] M. Frank and P. Wolfe, *An algorithm for quadratic programming*, Naval Res. Logist. Quart., 3 (1956), pp. 95–110.
[30] E. Haber, L. Horesh, and L. Tenorio, *Numerical methods for experimental design of large-scale linear ill-posed inverse problems*, Inverse Problems, 24 (2008), pp. 055012, 17.
[31] R. Herzog and I. Riedel, *Sequentially optimal sensor placement in thermoelastic models for real time applications*, Optim. Eng., 16 (2015), pp. 737–766.
[32] M. Hintermüller and K. Kunisch, *Feasible and noninterior path-following in constrained minimization with low multiplier regularity*, SIAM J. Control Optim., 45 (2006), pp. 1198–1221.
[33] M. Hintermüller and K. Kunisch, *Path-following methods for a class of constrained minimization problems in function space*, SIAM J. Optim., 17 (2006), pp. 159–187.
[34] M. Hintermüller, A. Schiela, and W. Wollner, *The length of the primal-dual path in Moreau-Yosida-based path-following methods for state constrained optimal control*, SIAM J. Optim., 24 (2014), pp. 108–126.
[35] M. Hinze, *A variational discretization concept in control constrained optimization: the linear-quadratic case*, Comput. Optim. Appl., 30 (2005), pp. 45–61.
[36] M. Jaggi, *Revisiting frank-wolfe: Projection-free sparse convex optimization*, in Proceedings of the 30th International Conference on International Conference on Machine Learning - Volume 28, ICML'13, JMLR.org, 2013, pp. I–427–I–435.

[37] J. Kiefer, *General equivalence theory for optimum designs (approximate theory)*, Ann. Statist., 2 (1974), pp. 849–879.
[38] J. Kiefer and J. Wolfowitz, *Optimum designs in regression problems*, Ann. Math. Statist., 30 (1959), pp. 271–294.
[39] S. Körkel, I. Bauer, H. G. Bock, and J. Schlöder, *A sequential approach for nonlinear optimum experimental design in DAE systems*, Scientific Computing in Chemical Engineering II, 2 (1999), pp. 338–345.
[40] A. Milzarek and M. Ulbrich, *A semismooth Newton method with multidimensional filter globalization for l_1-optimization*, SIAM J. Optim., 24 (2014), pp. 298–333.
[41] A. Pázman, *Foundations of optimum experimental design*, vol. 14 of Mathematics and its Applications (East European Series), D. Reidel Publishing Co., Dordrecht, 1986. Translated from the Czech.
[42] K. Pieper, *Finite element discretization and efficient numerical solution of elliptic and parabolic sparse control problems*, PhD Dissertation, Technische Universität München, 2015. `http://nbn-resolving.de/urn/resolver.pl?urn:nbn:de:bvb:91-diss-20150420-1241413-1-4`.
[43] K. Pieper, B. Q. Tang, P. Trautmann, and D. Walter, *Inverse point source location for the Helmholtz equation*, submitted.
[44] L. Pronzato, *Removing non-optimal support points in D-optimum design algorithms*, Statist. Probab. Lett., 63 (2003), pp. 223–228.
[45] F. Pukelsheim, *Optimal design of experiments*, Wiley Series in Probability and Mathematical Statistics: Probability and Mathematical Statistics, John Wiley & Sons, Inc., New York, 1993. A Wiley-Interscience Publication.
[46] A. Rakotomamonjy, R. Flamary, and N. Courty, *Generalized conditional gradient: analysis of convergence and applications*, ArXiv e-prints, (2015).
[47] W. Rudin, *Real and complex analysis*, McGraw-Hill Book Co., New York, third ed., 1987.
[48] R. C. St. John and N. R. Draper, *D-optimality for regression designs: a review*, Technometrics, 17 (1975), pp. 15–23.
[49] G. Stadler, *Elliptic optimal control problems with L^1-control cost and applications for the placement of control devices*, Comput. Optim. Appl., 44 (2009), pp. 159–181.
[50] E. Steinitz, *Bedingt konvergente Reihen und konvexe Systeme. (Fortsetzung)*, J. Reine Angew. Math., 144 (1914), pp. 1–40.
[51] A. Tarantola, *Inverse problem theory and methods for model parameter estimation*, Society for Industrial and Applied Mathematics (SIAM), Philadelphia, PA, 2005.
[52] F. Tröltzsch, *Optimal control of partial differential equations*, vol. 112 of Graduate Studies in Mathematics, American Mathematical Society, Providence, RI, 2010. Theory, methods and applications, Translated from the 2005 German original by Jürgen Sprekels.
[53] D. Uciński, *Optimal measurement methods for distributed parameter system identification*, Systems and Control Series, CRC Press, Boca Raton, FL, 2005.
[54] M. Ulbrich, *Semismooth Newton methods for operator equations in function spaces*, SIAM J. Optim., 13 (2002), pp. 805–842 (2003).
[55] B. Vexler, *Adaptive finite element methods for parameter identification problems*, PhD Dissertation, Ruprecht-Karls-Universität Heidelberg, 2004. `http://www.ub.uni-heidelberg.de/archiv/4603`.
[56] P. Wolfe, *Convergence theory in nonlinear programming*, North-Holland, Amsterdam, 1970.
[57] H. P. Wynn, *The sequential generation of D-optimum experimental designs*, Ann. Math. Statist., 41 (1970), pp. 1655–1664.
[58] Y. Yu, *D-optimal designs via a cocktail algorithm*, Stat. Comput., 21 (2011), pp. 475–481.

Institut für Numerische Simulation, Universität Bonn, Wegelerstr. 6, 53115 Bonn, Germany
E-mail address: `neitzel@is.uni-bonn.de`

Dept. Scientific Computing, Florida State University, 400 Dirac Science Library, Tallahassee, FL 32306, USA
E-mail address: `kpieper@fsu.edu`

Center for Mathematical Sciences, Chair M17, Technische Universität München, Boltzmannstr. 3, 85748 Garching bei München, Germany
E-mail address: `vexler@ma.tum.de, walter@ma.tum.de`